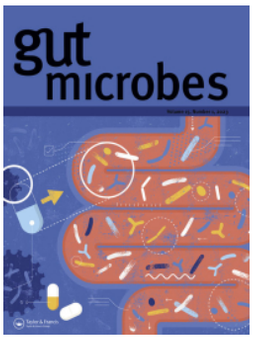

Gut Microbes

ISSN: (Print) (Online) Journal homepage: www.tandfonline.com/journals/kgmi20

Gut microbiota-mediated polyphenol metabolism is restrained by parasitic whipworm infection and associated with altered immune function in mice

Audrey Inge Schytz Andersen-Civil, Pankaj Arora, Ling Zhu, Laura J. Myhill, Nilay Büdeyri Gökgöz, Josue L. Castro-Mejia, Milla M. Leppä, Lars H. Hansen, Jacob Lessard-Lord, Juha-Pekka Salminen, Stig M. Thamsborg, Dennis Sandris Nielsen, Yves Desjardins & Andrew R. Williams

To cite this article: Audrey Inge Schytz Andersen-Civil, Pankaj Arora, Ling Zhu, Laura J. Myhill, Nilay Büdeyri Gökgöz, Josue L. Castro-Mejia, Milla M. Leppä, Lars H. Hansen, Jacob Lessard-Lord, Juha-Pekka Salminen, Stig M. Thamsborg, Dennis Sandris Nielsen, Yves Desjardins & Andrew R. Williams (2024) Gut microbiota-mediated polyphenol metabolism is restrained by parasitic whipworm infection and associated with altered immune function in mice, Gut Microbes, 16:1, 2370917, DOI: 10.1080/19490976.2024.2370917

To link to this article: https://doi.org/10.1080/19490976.2024.2370917

GUT MICROBES
2024, VOL. 16, NO. 1, 2370917
https://doi.org/10.1080/19490976.2024.2370917

Taylor & Francis
Taylor & Francis Group

Gut microbiota-mediated polyphenol metabolism is restrained by parasitic whipworm infection and associated with altered immune function in mice

Audrey Inge Schytz Andersen-Civil[a#], Pankaj Arora[a#], Ling Zhu[a], Laura J. Myhill[a], Nilay Büdeyri Gökgöz[b], Josue L. Castro-Mejia[b], Milla M. Leppä[c], Lars H. Hansen[d], Jacob Lessard-Lord[e], Juha-Pekka Salminen[c], Stig M. Thamsborg[a], Dennis Sandris Nielsen[b], Yves Desjardins[e], and Andrew R. Williams[a]

[a]Department of Veterinary and Animal Sciences, University of Copenhagen, Frederiksberg, Denmark; [b]Department of Food Sciences, University of Copenhagen, Frederiksberg, Denmark; [c]Natural Chemistry Research Group, Department of Chemistry, University of Turku, Turku, Finland; [d]Department of Plant and Environmental Sciences, University of Copenhagen, Frederiksberg, Denmark; [e]Institute of Nutrition and Functional Foods (INAF), Laval University, Québec, QC, Canada

ABSTRACT

Polyphenols are phytochemicals commonly found in plant-based diets which have demonstrated immunomodulatory and anti-inflammatory properties. However, the interplay between polyphenols and pathogens at mucosal barrier surfaces has not yet been elucidated in detail. Here, we show that proanthocyanidin (PAC) polyphenols interact with gut parasites to influence immune function and gut microbial-derived metabolites in mice. PAC intake inhibited mastocytosis during infection with the small intestinal roundworm *Heligmosomoides polygyrus*, and altered the host tissue transcriptome at the site of infection with the large intestinal whipworm *Trichuris muris*, with a notable enhancement of type-1 inflammatory and interferon-driven gene pathways. In the absence of infection, PAC intake promoted the expansion of *Turicibacter* within the gut microbiota, increased fecal short chain fatty acids, and enriched phenolic metabolites such as phenyl-γ-valerolactones in the cecum. However, these putatively beneficial effects were reduced in PAC-fed mice infected with *T. muris*, suggesting concomitant parasite infection can attenuate gut microbial-mediated PAC catabolism. Collectively, our results suggest an inter-relationship between a phytonutrient and infection, whereby PAC may augment parasite-induced inflammation (most prominently with the cecum dwelling *T. muris*), and infection may abrogate the beneficial effects of health-promoting phytochemicals.

ARTICLE HISTORY
Received 13 February 2024
Revised 24 May 2024
Accepted 17 June 2024

KEYWORDS
Immune; Polyphenols; Parasite; Helminth; Microbiota

Introduction

Interest in the application of dietary phytonutrients as immunomodulatory and health-promoting dietary substances has been greatly increasing, due to rising rates of chronic autoimmune pathologies and antimicrobial drug resistance.[1] Proanthocyanidins (PAC) are plant-derived polyphenols, which are present in varying concentrations among commonly consumed foods, particularly grapes, berries and nuts.[2] Several studies have reported that PAC exhibit immunomodulatory properties, of which a common denominator is the downregulation of oxidative stress and aberrant inflammatory responses.[3–7] This may derive from direct modulation of antioxidant and inflammatory responses in gut epithelial and immune cells, as well as prebiotic effects whereby commensal gut bacteria metabolize PAC into phenolic metabolites that can improve gut barrier function,[8–10] or that are absorbed and subsequently exert systemic anti-inflammatory effects.[11–14]

The intestinal tract is continuously challenged by potential harmful stimuli, while balancing the proportion of commensal and opportunistic bacteria.[15,16] Therefore, the gut is one of the most immunologically active organs in the body, and the immune and inflammatory tone in the gut may impact not only responses to enteric pathogens but also inflammation and metabolism in extraintestinal tissues. The mucosal immune system contains discrete components that are specialized for combating specific infections, namely pro-

CONTACT Andrew R. Williams arw@sund.ku.dk Department of Veterinary and Animal Sciences, University of Copenhagen, Dyrlægevej 100, Frederiksberg DK-1870, Denmark
[#]Joint First Authors.
Supplemental data for this article can be accessed online at https://doi.org/10.1080/19490976.2024.2370917

inflammatory or type-1 responses against intracellular viruses and bacteria, and type-2 responses against multicellular parasitic worms (helminths). Dysregulation of these immune cell subsets can result in chronic disease such as Crohn's disease, which is an overactive type-1 response, or food allergies that are driven by overactive type-2 responses.[17,18]

Helminths are one of the most widespread pathogens of humans and animals, with around 1 billion people globally infected by different gastrointestinal-dwelling worms.[19] Further, these parasites are also ubiquitous in farmed livestock.[20] Under natural conditions, individuals are infected repeatedly with low-dose helminth infections throughout their lifetime, thus allowing the parasite to establish chronic, non-resolving infections.[21] When protective immunity to helminths develops, it is accompanied by type-2 immune mechanisms such as Th2 cells that produce IL-4 and IL-13, typically also accompanied by a strong T-regulatory component.[22] Murine infection models have established a clear paradigm that whilst enhancing the type-2 response increases resistance to helminths, strengthening of the type-1 response results in susceptibility to chronic infection.[21,23–25]

In contrast to the well-known effects of PAC on improving health during chronic metabolic diseases, it is not yet understood in detail how they impact immune function during pathogen infections. PAC-rich diets have shown modulatory effects on the immune response to helminth infections in livestock (sheep and pigs), including a boosting of infection-induced γδ T-cells, eosinophils, and antibodies.[26,27] However, PAC-enriched diets have also been shown to exacerbate infection with the extracellular bacterium *Citrobacter rodentium* infection in mice, which may be due to PAC-induced changes in the GM or mucosal immune function.[28] Thus, the effects of PAC on enteric infections may vary depending on factors such as host species or basal GM. So far, no studies have investigated the influence of PAC on helminth infection in mouse models fed purified, semi-synthetic diets (SSD) with a defined chemical composition. This may represent a useful system to examine the interactions between PAC and gut pathogens, and to assess if PAC intake can modulate the polarization of the immune system toward either a type-1 or type-2 immune response in natural models of parasite infection.

Here, we explored if the addition of PAC to purified, open-source murine diets can alter the immune response during enteric parasitic infection. We utilized two parasite systems, the small intestinal *Heligmosomoides polygyrus* and the large intestinal *Trichuris muris*, which can be used to effectively model the infection dynamics typically seen in natural infections in humans and animals.[22,29] We show that in both infection models PAC induces a modulation of the immune response induced by infection. Moreover, infection tended to modulate PAC-induced changes in the gut microbiome. Importantly, whilst PAC intake increased the abundance of microbial-derived metabolites positively associated with gut health, concurrent *T. muris* infection impaired production of such metabolites. Thus, our results point to an interaction between enteric parasite infection and dietary phytonutrients that may, in some contexts, negatively affect host health.

Results

Proanthocyanidins alter expression of immune-related genes and reduce mastocytosis during small intestinal nematode infection

To study if PAC can modulate mucosal immune responses to an enteric helminth infection, we first examined the effects of PAC intake on the small intestinal mucosal immune response to *H. polygyrus*. Mice were fed SSD (Supplementary Table S1) and were gavaged every 2nd day with 200 mg/kg purified PAC derived from grape pomace dissolved in water, or water only, for 4 weeks. Halfway through the experiment, mice in each treatment group were infected with *H. polygyrus* and euthanized 14 days post-infection (p.i.,), i.e., 28 days after initiation of PAC administration, or remained as uninfected controls (Figure 1a). RNA-sequencing (RNA-Seq) of duodenum tissues from *H. polygyrus*-infected mice without PAC intake showed a strong upregulation of many genes involved in type-2 immunity, relative to uninfected control mice (Figure 1b; Supplementary File 1). These included genes involved in mast cell responses, including mast cell proteases (*Mcpt1*,

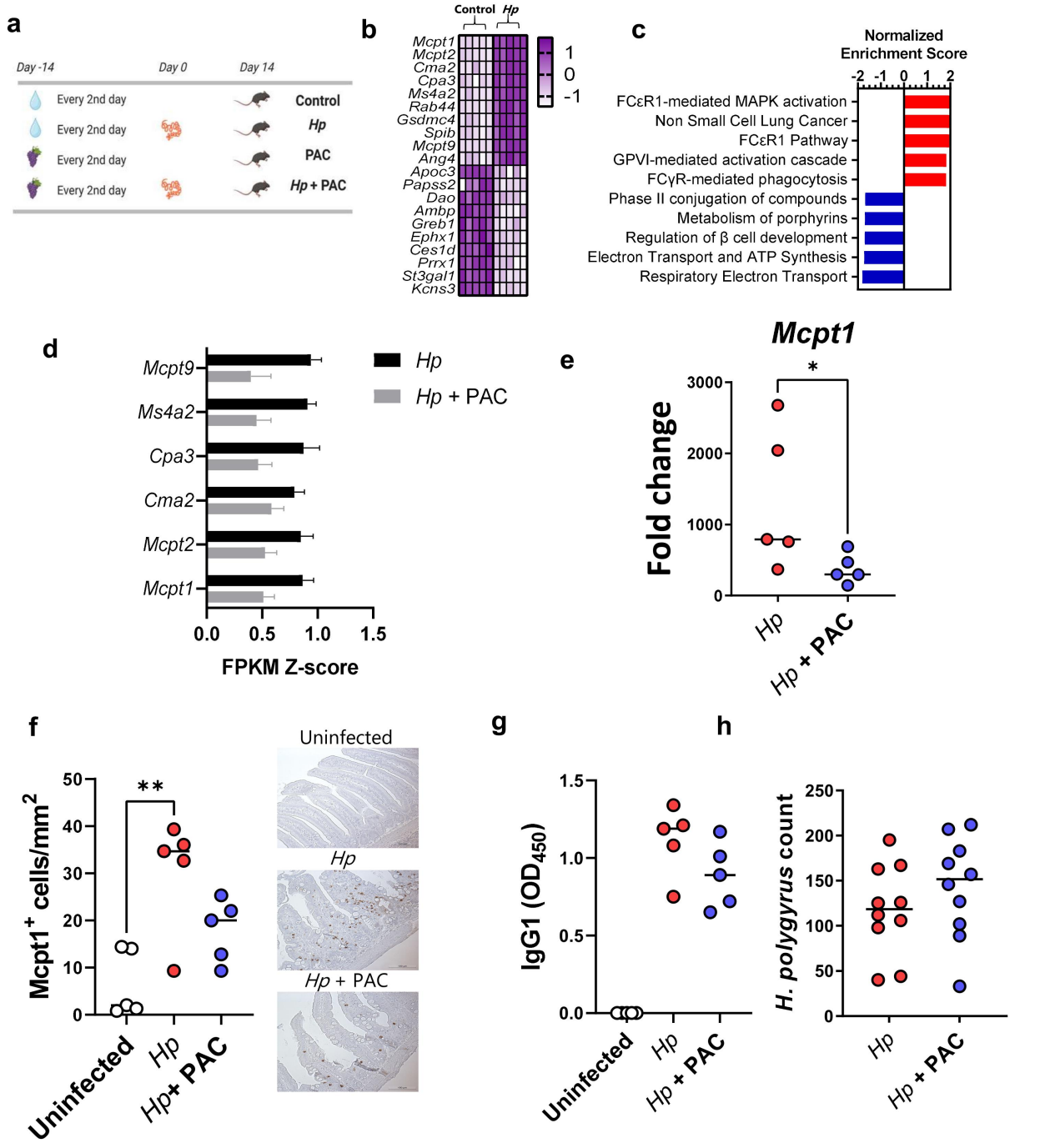

Figure 1. Proanthocyanidins downregulate immune-related genes and affect immune cell hyperplasia in duodenum tissues of Heligmosomoides polygyrus-infected mice with no effect on worm burdens. a) Schematic of experimental design. Mice in proanthocyanidin (PAC)-treated groups received 200 mg/kg PAC derived from grape pomace every 2nd day, whilst control mice received water. Mice infected with *H. polygyrus* (*Hp*) were inoculated with 200 larvae on day 0. b) Top ten up- and down-regulated genes (Z-scores) in the duodenum of *H. polygyrus*-infected mice relative to uninfected control mice, identified by RNA-sequencing (for all genes adjusted p value < 0.05 by DeSeq2). c) Top 5 up- and down-regulated gene pathways (q value < 0.05) in duodenal tissue identified by gene set enrichment analysis in mice infected with *H. polygyrus*, relative to uninfected mice. d) Specific expression of mast cell-related genes in the duodenum of *H. polygyrus*-infected mice and PAC-dosed *H. polygyrus*-infected mice, relative to uninfected control mice. Shown are means ± S.E.M. of FPKM values from RNA-Seq analsyis. e) Expression of *Mcpt1* as measured by qPCR. Fold changes are relative to uninfected, control mice. Shown are median values. f) Enumeration of Mcpt1-positive mast cells in the duodenum. Shown are median values. g) *H. polygyrus*-specific serum IgG1 levels in serum. Shown are median values. h) Worm burdens in *H. polygyrus*- infected mice with and without PAC treatment. Shown are median values. A)-G), $n = 5$ per treatment group from a single experiment, H) $n = 10$ per group, pooled from two independent experiments. *$p < 0.05$, **$p < 0.01$, by Mann-Whitney tests or Kruskal-Wallis tests with Dunn's post-hoc testing.

Mcpt2), chymases (*Cma2*) and subunits of the high-affinity IgE receptor (*Ms4a2*). Furthermore, innate defense molecules (e.g., *Ang4*) were upregulated (Figure 1b). Downregulated genes were mainly involved in nutrient uptake and metabolism, consistent with the marked changes in gut function that accompany *H. polygyrus* infections.[30] Transcriptional pathways enriched by *H. polygyrus* infection were mainly related to mastocytosis, whilst suppressed pathways were connected to metabolic processes such as electron transfer, ATP synthesis and cellular biotransformation (Figure 1c). Thus, *H. polygyrus* infection induced a strong modulatory effect on the intestinal environment with marked upregulation of type-2 immune mechanisms, and a suppression of cellular metabolism that may relate to mucosal injury and necrosis induced by nematode invasion of the host tissue.

In contrast, PAC intake in uninfected mice did not substantially change the duodenal transcriptome, with no significantly regulated genes following multiple correction testing (Supplementary File 2). PAC do therefore not seem to have a strong effect at this tissue site, at least in parasite-naïve mice. To explore if PAC intake impacted on host responses during *H. polygyrus* infection, we next compared duodenal transcriptomic responses of *H. polygyrus*-infected mice receiving either PAC or water alone. Overall, PAC had only minor effects on the transcriptional response to *H. polygyrus* infection. However, we noted suppression of several genes by PAC that were related to mast cell or immunoglobulin signaling, such as *Mcpt1* and *Ms4a2*, albeit again not significantly so after correction for multiple testing (Supplementary Figure S1; Supplementary File 3). Indeed, expression of the top mast cell related genes identified as being upregulated by *H. polygyrus* in Figure 1a was noticeably lower in infected mice administered PAC, relative to infected controls (Figure 1d). Given the lack of statistical significance from RNA-Seq analysis, we verified the suppression of the mast cell response in several ways. qPCR confirmed that infection-induced upregulation of *Mcpt1* was significantly attenuated by PAC, and Mcpt1^{+} mast cells in the intestinal mucosa were significantly elevated by infection in infected control-fed mice but not in infected mice administered PAC (Figure 1e–f). However, we observed no significant effect of PAC on *H. polygyrus*-specific IgG1 levels in serum or worm burdens at day 14 p.i., (Figure 1g–h). Thus, in this model dietary PAC supplementation did not significantly enhance parasite-specific immunity, but rather tended to restrain mast cell responses induced by *H. polygyrus*, although worm counts remained unchanged.

Proanthocyanidins modulate caecal transcriptomic responses during Trichuris muris infection

To further investigate the effect of PAC intake on helminth-specific immune function, we utilized a second infection model, the cecal dwelling whipworm *T. muris*. We have previously shown that a trickle infection with low doses of *T. muris* eggs in SSD-fed mice leads to a mixed type-1 and type-2 immune response, which results in expulsion of the majority of the worms within 4–5 weeks but leaves a small residual adult worm burden, along with the development of sporadic colitis-like pathology.[31] Thus, this infection regime is well-suited for testing whether PAC intake may affect the polarization of the naturally-induced anti-helminth immune response. Furthermore, the location of *T. muris* in the cecum, the main site of fermentation of diet-derived plant material in mice, may make this model particularly relevant for assessing interactions with dietary components, given that PAC consumption has been previously shown to modulate gene expression and gut barrier activity in the cecum and colon.[32,33]

Mice trickle infected with *T. muris* (3 doses of 20 eggs over 35 days), and uninfected controls, received oral administration of purified PAC from grape seed extract (300 mg/kg) 14 days prior to, and throughout, the infection period (Figure 2a). Interestingly, PAC intake decreased body weight gains relative to mice consuming only SSD (Supplementary Figure S2). Using RNA-Seq, we first characterized the transcriptional response in cecum tissue to *T. muris* infection alone. Relative to uninfected controls, *T. muris*-infected mice had altered the expression of more than 2000 genes (adjusted $p < 0.05$; Fold change ≥ 2). Similar to *H. polygyrus* infection, mast-cell related genes such as *Mcpt1* were strongly upregulated but were accompanied by pronounced upregulation of

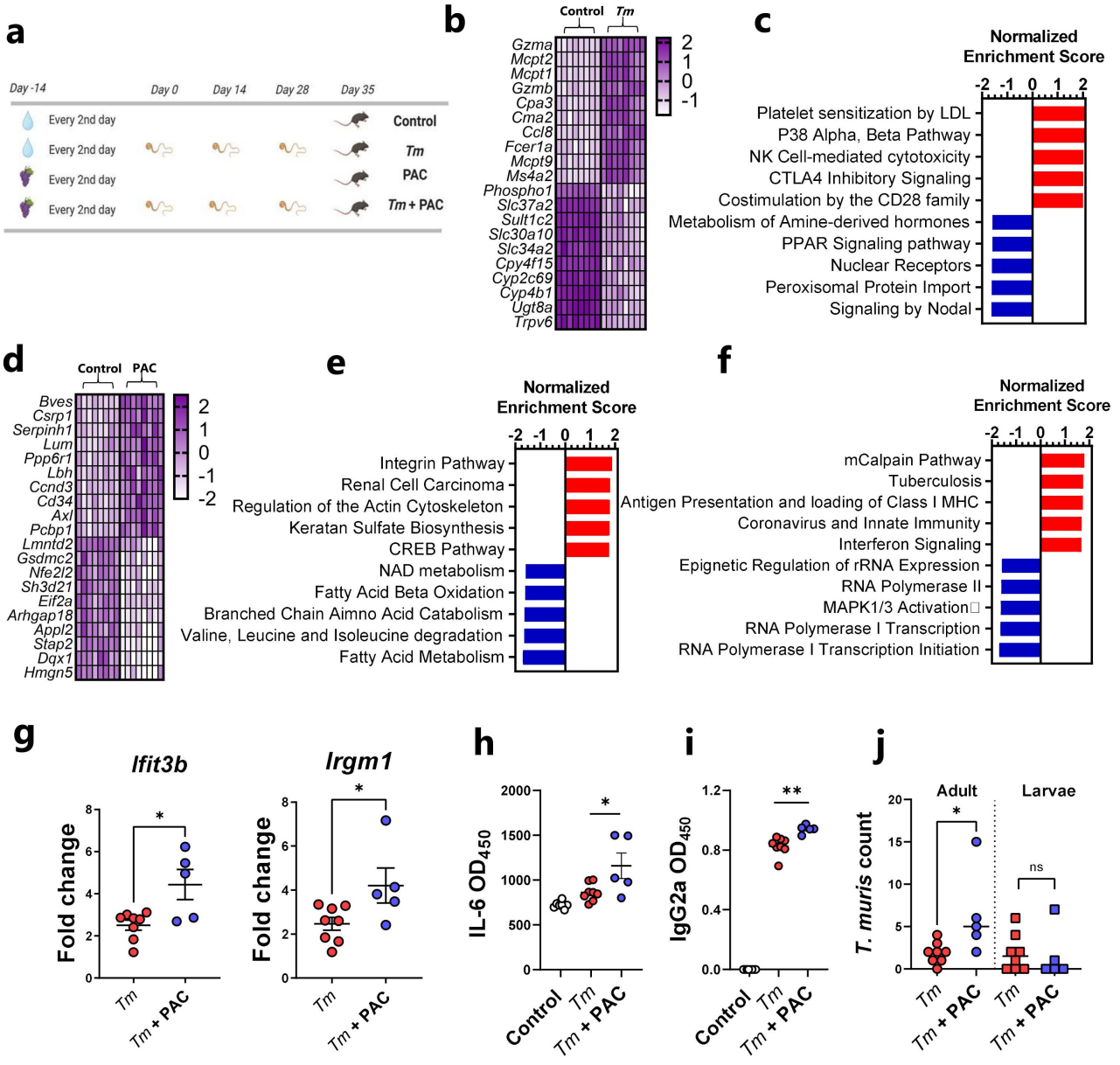

Figure 2. Proanthocyanidins modulate immune responses in Trichuris muris-infected mice. a) Schematic of experimental design. Mice in proanthocyanidin (PAC)-treated groups received 300 mg/kg PAC derived from grape seeds every 2nd day, whilst control mice received water. Mice infected with *Trichuris muris* (*Tm*) were inoculated with 20 eggs on day 0, 14 and 28. b) Top ten up- and down-regulated genes (Z-scores) in the cecum of *T. muris*-infected mice relative to uninfected control mice, identified by RNA-sequencing (for all genes adjusted p value < 0.05 by DeSeq2). c) Top 5 up- and down-regulated gene pathways (q value < 0.05) in cecal tissue identified by gene set enrichment analysis in mice infected with *T. muris*, relative to uninfected mice. d) Top ten up- and down-regulated genes (Z-scores) in the cecum of PAC-dosed mice relative to water-dosed control mice, identified by RNA-sequencing (for all genes adjusted p value < 0.05 by DeSeq2). e) Top 5 up- and down-regulated gene pathways (q value < 0.05) in cecal tissue identified by gene set enrichment analysis in PAC-dosed mice relative to water-dosed control mice. f) Top 5 up- and down-regulated gene pathways (q value < 0.05) in cecal tissue identified by gene set enrichment analysis in PAC-dosed mice infected with *T. muris*, relative to mice infected with *T. muris* alone. g) Expression of *Ifit3b* and *Irgm1* measured by qPCR. Fold changes are relative to uninfected, control mice. h) IL-6 induced by *T. muris* antigens in lymphocytes isolated from mesenteric lymph nodes in *T. muris*-infected mice, with or without PAC dosing. i) *T. muris*-specific serum IgG2a levels in serum. J) Adult and larval worm burdens in *T. muris*-infected mice For all panels, n = 5-8 per group, pooled from two independent experiments. g) – h) – Shown are means ± S.E.M. *p < 0.05 by un-paired t test. I) – j) – Shown are median values. *p < 0.05, **p < 0.01 by Mann-Whitney test.

Gzma, *Ifng*, and *Nos2*, suggesting a mixed type-1/type-2 response (Figure 2b; Supplementary File 4). Consistent with this, gene pathways indicative of pro-inflammatory response (NK cell signaling, CD28 signaling) were strongly enriched, whilst metabolic pathways connected to hormone and peroxisome proliferator-activated receptor (PPAR) signaling were amongst the most suppressed (Figure 2c). Thus, *T. muris* trickle infection induced significant cecal inflammation and disruption of metabolic homeostasis in the gut.

As a first step in determining whether PAC intake could modulate this response, we first carried out a similar RNA-Seq approach to determine transcriptional responses in cecal tissue of uninfected mice fed PAC to establish a baseline profile of the effect of PAC administration. Most of the upregulated genes resulting from PAC intake (e.g. *Bves, Csrp1, Cd34*) were related to cell adhesion and differentiation, which was supported by the enrichment of gene pathways related to integrins, cell proliferation, and extracellular matrix remodeling (Actin, Keratan sulfate activity), consistent with known functions of PAC in stimulating epithelial cell growth[34] (Figure 2d–e; Supplementary File 5). Interestingly, PAC intake was associated with down-regulation of *Nfe2l2*, encoding the transcription factor Nrf2, supporting a role in modulation of oxidative stress responses, as well as *Gsdmc2*, encoding the epithelial cell protein gasdermin-2 which may be involved with cell lysis and pyroptosis.[35] Downregulated gene pathways were mainly related to metabolic function such as fatty acid metabolism, coherent with known roles of PAC in regulating lipid and bile acid metabolism.[36] Thus, PAC intake, in the absence of infection, was associated with modulation of transcriptional pathways putatively associated with tissue remodeling and nutrient metabolism, suggesting that PAC has significant effects on the local mucosal environment in the large intestine.

Next, cecal tissues harvested from *T. muris*-infected mice administered PAC were compared to cecal tissues from mice infected with *T. muris* without PAC treatment. Notably, despite the differences in tissue type and infection dynamics we observed a similar picture to that observed with *H. polygyrus*. Specifically, only minor gene expression changes were induced by PAC, relative to water-dosed controls, with no genes being significantly changed after correction for multiple testing (Supplementary Figure S3; Supplementary File 6). However, when considering genes upregulated by PAC with unadjusted p values of < 0.005, it was again notable that some of these (e.g. *Ifit3b* and *Irgm1*) were related to a shift from a type-2 to a type-1 immune environment in the infected tissue (Supplementary Figure S3). Thus, we explored in greater detail if PAC modulated the host response to *T. muris*. First, we conducted gene-set enrichment analysis, which revealed significant ($q < 0.05$) up-regulation of several pathways related to either interferon production or immune responses toward viral or bacterial pathogens, in PAC-dosed mice during *T. muris* infection (Figure 2f). Next, we confirmed by qPCR that the expression of *Ifit3b* and *Irgm1*, both encoding proteins downstream of IFNγ production, was significantly increased in the cecal tissue of *T. muris*-infected mice fed PAC, relative to *T. muris* alone (Figure 2g). We then analyzed serum antibodies and cytokine production from mesenteric lymph node (MLN) cells. Infected mice fed PAC had significantly increased serum levels of *T. muris*-specific IgG2a, a marker of type-1 responses and parasite chronicity[29] (Figure 2h). Whilst MLN cytokine secretion induced by *T. muris* antigen was largely similar between both groups (Supplementary Figure S4), we noted significantly higher IL-6 production in infected mice fed PAC (Figure 2i). Finally, adult worm burdens were significantly higher in PAC-treated mice, but larval and total worm burdens were not different (Figure 2j). To test further whether PAC could impair the ability of the host to expel *T. muris*, we employed a high-dose infection regime where mice were infected with a single dose of 300 *T. muris* eggs, which typically results in rapid clearance of the infection by day 21 p.i. Consistent with this, mice fed the SSD control diet had very few worms at day 21 following a high-dose infection. This ability to expel the infection was not impaired by concurrent PAC intake, and *T. muris*-specific IgG2a in serum was also not affected (Supplementary Figure S5). This suggests that the immunomodulatory effects of PAC are not sufficient to impair the ability of the host to remove the worms. Taken together, these data are consistent with the *H. polygyrus* model and indicate that PAC selectively modulates elements of the response elicited by parasitic infection, such as IL-6 production from MLN.

Thus, despite PAC intake having seemingly beneficial effects on the mucosal barrier in uninfected mice, PAC intake during *T. muris* infection did not lower worm burdens and was instead associated with increased production of some pro-inflammatory elements of the immune response during trickle infection.

Proanthocyanidins alter T cell populations in mesenteric lymph nodes in helminth-infected mice

The balance between differentiated intestinal T-cells during helminth infection may play a key role in determining the outcome of infection.[37] To explore if the transcriptomic changes observed in mucosal gut tissues were accompanied by changes in T-cell populations, MLN were isolated from *H. polygyrus*-infected mice at day 14 p.i. and from *T. muris*-infected mice at day 35 p.i. to assess how these were altered by infection and/or PAC supplementation. Interestingly, PAC intake significantly increased the total number of cells in the MLN of both infection models, relative to infected mice which were not administered PAC (Figure 3a). PAC had no effect on the proportions of Th1 ($Tbet^+$), Th2 ($GATA3^+$) and $Foxp3^+$ T-helper cells within the T-helper cell population ($TCR\beta^+CD4^+$) in uninfected mice (data not shown). In *H. polygyrus*-infected mice, proportions of Th1 cells were not affected by PAC, but, interestingly, the proportion of Th2 cells was significantly increased (Figure 3b), in contrast to the mast cell data overserved previously. However, we also noted a strong tendency for the proportion of Treg cells to also be increased by PAC (Figure 3b). In contrast, PAC intake in *T. muris*-infected mice did not result in significant changes in the proportions of MLN T-cell subsets (Figure 3c). Thus, PAC supplementation had a stimulatory effect on lymphocyte proliferation in the MLN during helminth infection, and the relative expansion of different T-cell subsets was highly dependent on infection model.

Proanthocyanidins modulate immune responses during Trichuris muris infection more strongly with semi-synthetic diets than with chow

Previous studies have shown that inclusion of plant-derived oligosaccharides in SSD, but not unrefined mouse chow, can exacerbate colitis and inflammation,[38] suggesting that basal diet may play a role in dictating how phytochemicals modulate gut inflammation. Given that PAC seemed to modulate the response to *T. muris* trickle infection in mice fed SSD, we explored if this was dependent on the dietary matrix that accompanied PAC administration. Mouse chow is a crude mixture containing many components including lignins, non-starch polysaccharides, and isoflavones. In contrast, SSD are essentially free of phytonutrients, containing mainly purified casein, starch, sucrose and cellulose (Supplementary Table S1). We thus hypothesized that the immunomodulatory effects of PAC would be more pronounced when administered together with SSD, than with mouse chow. Mice were trickle-infected with *T. muris* as above, and fed either chow or SSD, with or without 300 mg/kg purified PAC from grape seed extract every 2nd day. In line with our previous results, mice dosed with PAC gained less weight, and this was most pronounced in the SSD-fed mice (Figure 4a). The pattern of worm burdens was similar to what we previously observed, although no significant differences were found. Strikingly, consistent with our recent observations,[31] basal diet composition had a marked effect on *T. muris* burdens with a substantial increase in both adults and larvae in chow-fed mice, compared to SSD-fed mice (Figure 4b,c). There was also a significant increase in MLN cells in chow-fed mice compared to SSD-fed mice (Figure 4d). PAC administration did not significantly change the proportions of Th1 cells in the MLN compared to controls but did reduce the proportion of Th2 cells, most prominently in the SSD-fed mice ($p = 0.06$ for interaction between diet and infection; Figure 4e,f). Thus, there was a significantly skewed Th1:Th2 ratio in SSD-fed mice ($p < 0.05$ for interaction between basal diet and PAC intake; Figure 4g). IgG2a levels were also markedly affected by basal diet, with higher levels in chow-fed mice, correlating with worm burden, with no significant effect of PAC (Figure 4h). Finally, we quantified *T. muris* antigen-induced IL-6 secretion in MLN cells and found increased levels in PAC-dosed mice, but again only when fed SSD and not chow ($p < 0.05$ for interaction between basal diet and PAC intake; Figure 4i). Collectively, these data demonstrate that basal diet composition has a substantial effect on worm burden and immune responses, and that modulation of T-cell

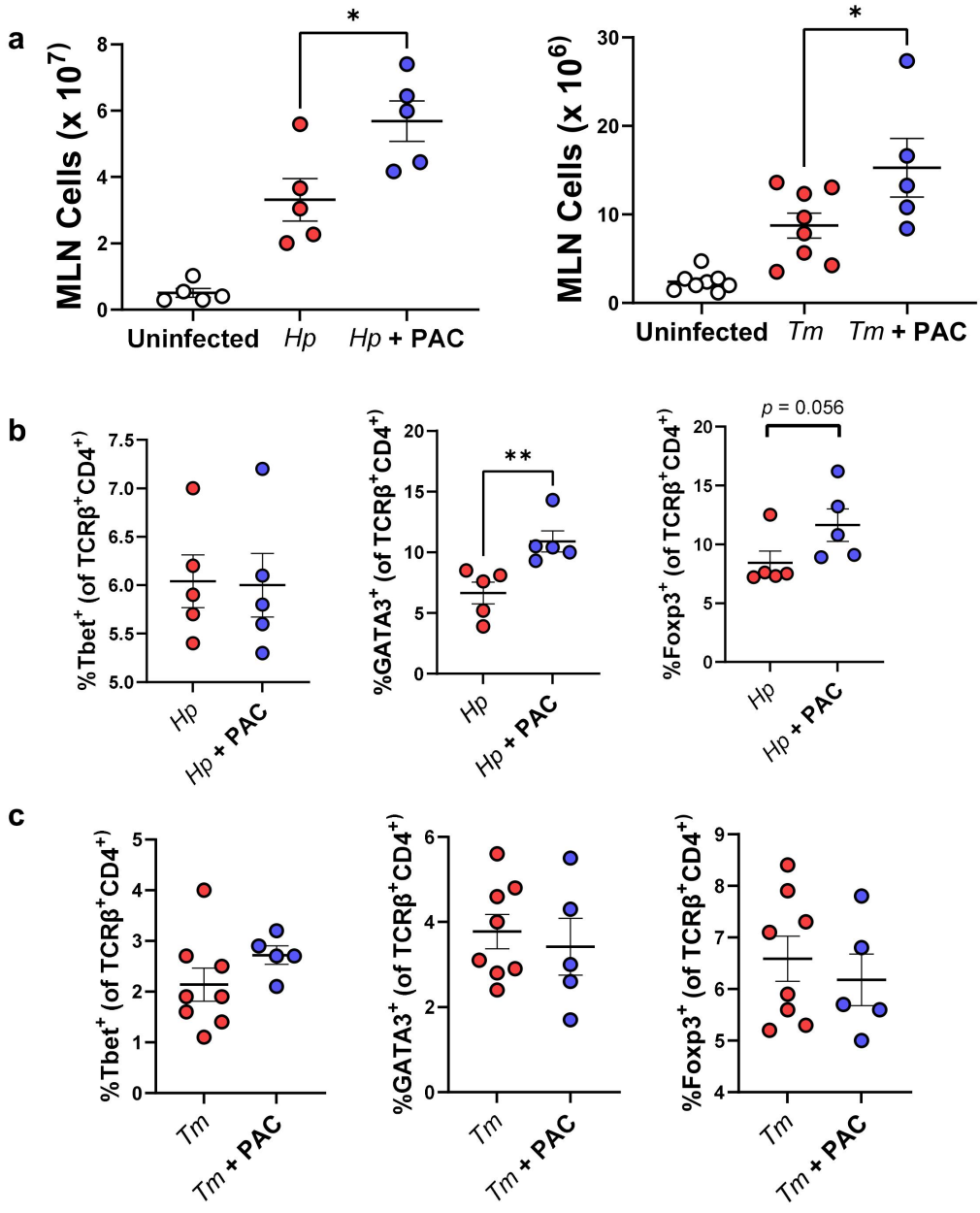

Figure 3. Proanthocyanidins alter T cell populations in the mesenteric lymph nodes in helminth-infected mice. Impact of proanthocyanidins (PAC) on the total number of cells (a), and proportions of TCRβ$^+$ CD4$^+$T-bet$^+$, TCRβ$^+$ CD4$^+$GATA3$^+$ and TCRβ$^+$ CD4$^+$Foxp3$^+$ T-cells in the mesenteric lymph nodes (MLN) of *Heligmosomoides polygyrus* (*Hp*; B) and and *Trichuris muris* (*Tm*; C) infected mice. b) $n = 5$ per treatment group from a single experiment. c) $n = 5$-8 per group, pooled from two independent experiments. Shown are means ± S.E.M. * $p<0.05$ by unpaired t-test. Gating strategy is shown in Supplementary Figure 8.

responses and IL-6 production in MLN during *T. muris* infection is more strongly influenced by PAC when mice are fed SSD than chow.

Proanthocyanidins and helminths interact to change gut microbiota composition

We next assessed if PAC intake and/or helminth infection influenced GM composition. In the *H. polygyrus* infection model, PAC intake significantly increased α-diversity in the cecal microbiota based on the number of observed zOTUs, but not on Shannon diversity index, whilst *H. polygyrus* infection had no effect on these measures (Figure 5a). Pairwise PERMANOVA analysis assessing cecal microbiota compositional differences (Bray-Curtis dissimilarity based) revealed a clear

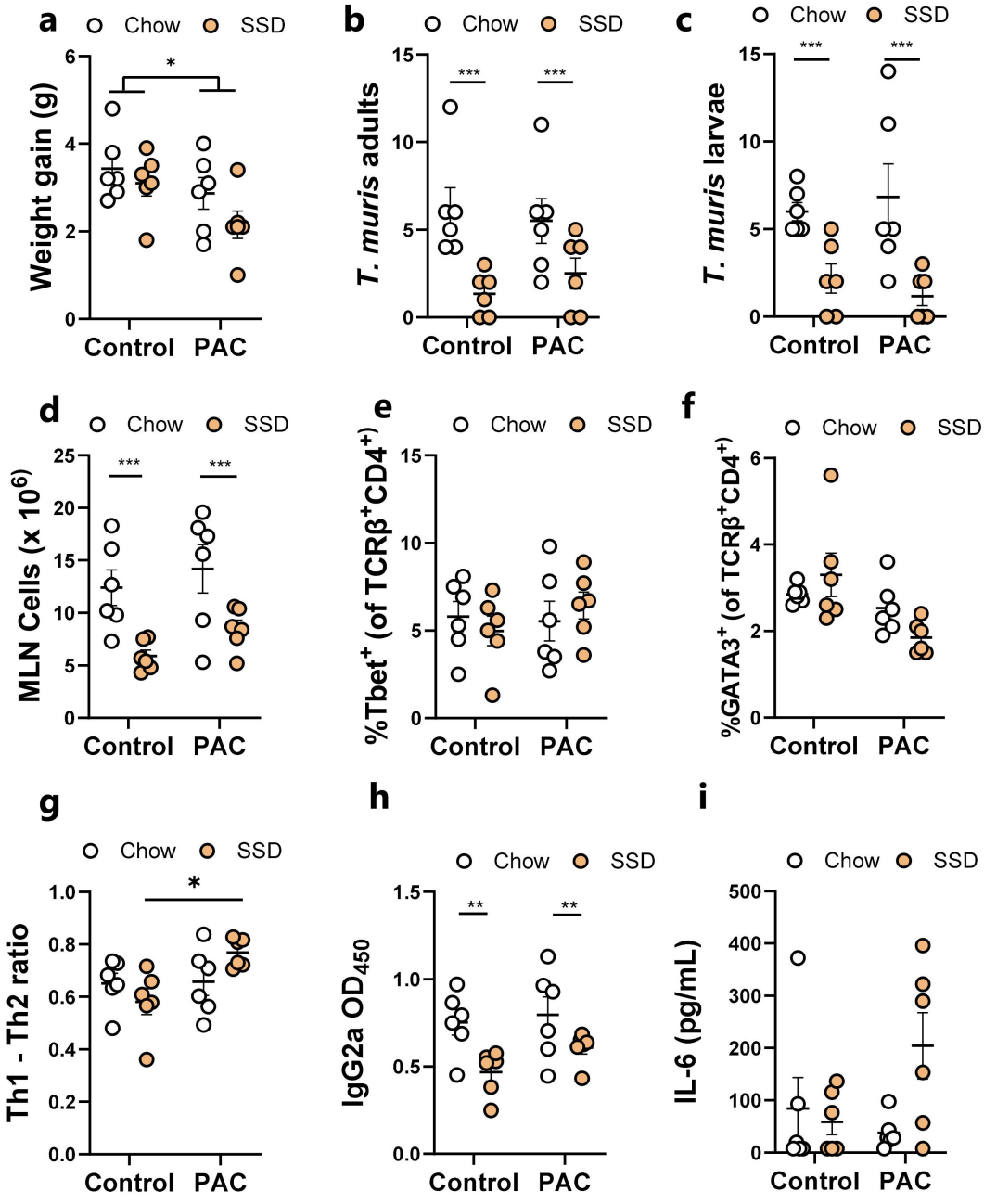

Figure 4. Effects of proanthocyanidins during Trichuris muris infection in mice fed either chow or semi-synthetic diets. a) Weight gain over the course of the 49 day experiment in mice fed either chow or semi-synthetic diets (SSD), and administered either proanthocyanidins (PAC) or water (control). Adult and larval *T. muris* counts (b-c), total cellularity of the mesenteric lymph nodes (d), proportions of T-bet$^+$ (Th1) and GATA3$^+$ (Th2) cells within the MLN TCRβ$^+$ CD4$^+$ population, and the Th1/Th2 ratio (e-g), serum IgG2a specific for *T. muris* antigen (h), and IL-6 secretion from MLN cells stimulated with *T. muris* antigen (i) at day 35 following the start of *T. muris* infection. $n = 6$ per treatment group from a single experiment. *$p < 0.05$, **$p < 0.01$, ***$p<0.005$ by two-way ANOVA with Tukey post-hoc testing. Shown are means ± S.E.M.

interaction between *H. polygyrus* infection and PAC intake, whereby the effect of PAC was modulated by concurrent infection. In uninfected mice, the cecal microbiome composition was significantly different in mice fed PAC relative to the control diet (adjusted $p < 0.05$; Figure 5b). In contrast, PAC had no effect in *H. polygyrus*-infected mice (adjusted $p > 0.05$), indicating that infection abrogated the effects of PAC intake on the cecal microbiome composition. In contrast, regardless of

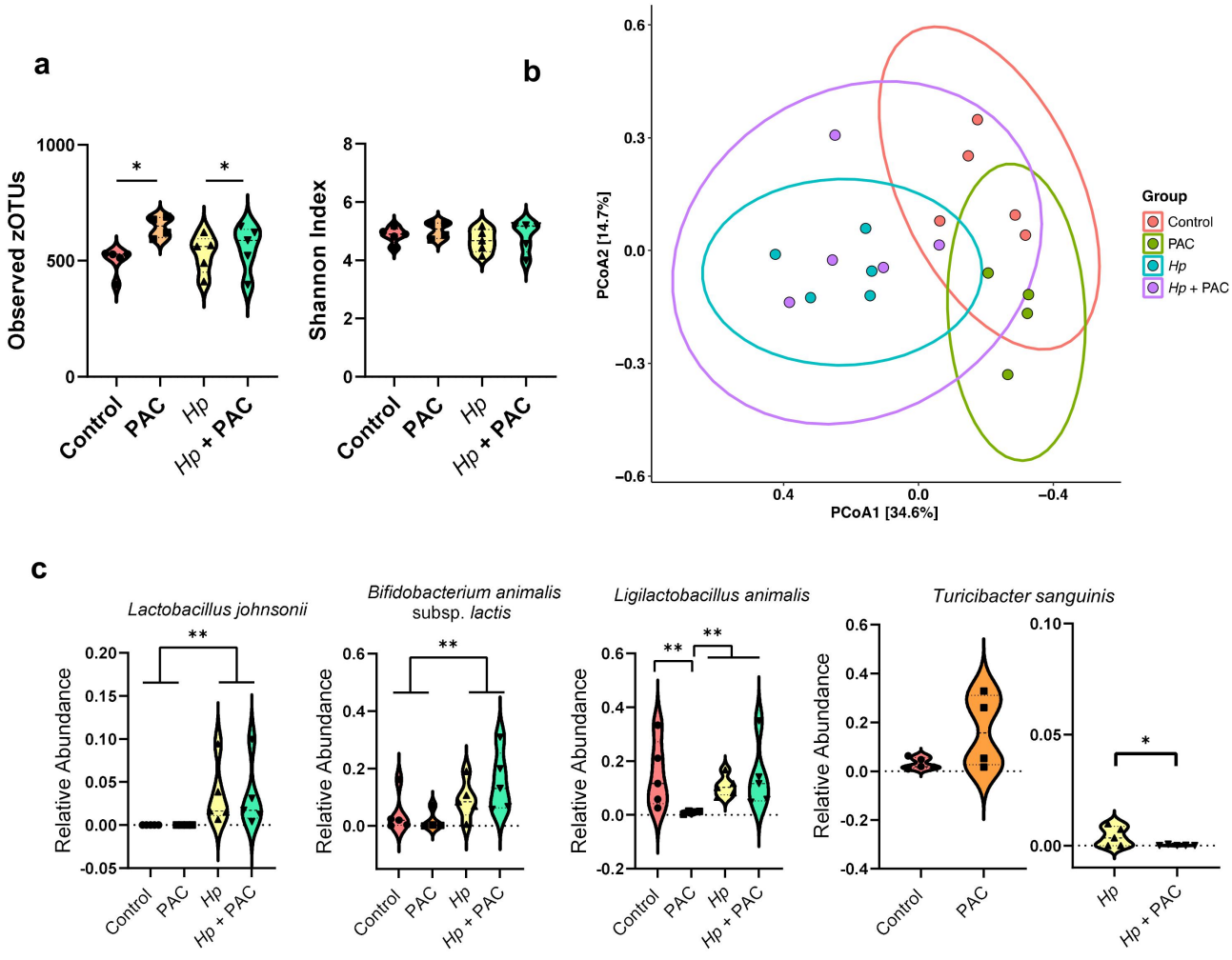

Figure 5. Impact of Heligmosomoides polygyrus (Hp) infection and proanthocyanidins (PAC) on the host cecal microbiota. a) Violin plots illustrating the number of observed zOTUs and Shannon Diversity Index for each treatment group. * $p < 0.05$ by two-way ANOVA followed by Tukey post-hoc testing. Shown is median and interquartile range. B) Principal coordinates analysis based on Bray-Curtis dissimilarity metrics for control and *Hp*-infected mice fed with semi-synthetic diets and dosed with either PAC or water (control). Each data point on the PCoA plots indicate a sample, with ellipses showing 95% confidence interval. The percentage in brackets is the percentage of variation explained by each PCoA axis. Pairwise comparisons between treatment groups were performed using permutation MANOVAs on a distance matrix with p-value correction using the Holm method. $p<0.05$ was considered as significant. C) Relative abundance violin plots for zOTUs corresponding to *Lactobacillus johnsonii*, *Turicibacter sanguinis*, *Ligilactobacillus animalis*, and *Bifidobacterium animalis* subsp. *lactis* in uninfected and *Hp*-infected mice dosed with either PAC or water (control) ($n = 4$-5 per treatment group). The significance of difference was assessed by two-way ANOVA and Tukey post-hoc testing (* $p<0.05$; ** $p < 0.01$). Shown is median and interquartile range.

PAC intake, *H. polygyrus* infection resulted in significant changes in the cecal microbiome composition relative to uninfected mice, (adjusted $p < 0.05$; Figure 5b). Pairwise DESeq2 analysis identified 10 and 12 species that were impacted by *H. polygyrus* infection in control- and PAC-dosed mice, respectively (Supplementary Figure S6). Similar to previous studies,[39,40] the major change induced by *H. polygyrus* was an increase in lactobacilli, predominately *Lactobacillus johnsonii*, and *Bifidobacterium animalis* subsp. *lactis* ($p < 0.05$ for main effect of infection by two-way ANOVA; Figure 5c). In uninfected mice, PAC intake resulted in three differentially abundant taxa by DESeq2, these being a reduction in the relative abundance of *Ligilactobacillus animalis* and increases within unclassified members of the *Gordonibacter* and *Corynebacterium* members (Supplementary Figure S5). Moreover, PAC intake tended to increase (adjusted $p = 0.06$ by DESeq2) the abundance of *Turicibacter sanguinis*, a bacterium associated with altered fat digestion and reduced triglyceride

levels,[41] consistent with reported effects of PAC-rich diets on lipid metabolism.[42] However, these effects of PAC were strongly influenced by concurrent *H. polygyrus* infection, with relative *L. animalis* abundance not affected by PAC in infected mice (Figure 5c). Moreover, infection strongly suppressed *T. sanguinis* abundance and completely abrogated the PAC-induced increase in *T. sanguinis*. Indeed, within *H. polygyrus*-infected mice, *T. sanguinis* relative abundance was significantly lower in PAC-dosed mice ($p < 0.05$ for interaction between diet and infection by two-way ANOVA; Figure 5c). Collectively, these data indicate that PAC-induced changes in GM composition were attenuated by concurrent *H. polygyrus* infection.

In fecal samples of *T. muris*-infected mice (35 days post-infection), infection had the strongest effect on GM composition. Infected mice had significantly lower α-diversity (both in terms of observed zOTUs and Shannon index metrics), whilst PAC had no effect (Figure 6a). The fecal microbiome compositions of infected mice tended to diverge from uninfected mice, regardless of PAC intake (adjusted $p = 0.08$ for effect of infection in both control-fed and PAC-fed mice by pairwise PERMANOVA on Bray-Curtis dissimilarity metrics; Figure 6b). DESeq2 analysis indicated that infection changed the abundance of 15 and 17 species in control and PAC-dosed mice, respectively (Supplementary Figure S7). Notably, when comparing the overall effect of infection (irrespective of PAC intake) there was a significant increase in *Li. animalis* abundance, consistent with previous studies showing an expansion in lactobacilli in mice with a chronic *T. muris* infection.[43] We did not observe a significant effect of PAC on fecal GM composition (adjusted $p = 0.3$ by pairwise PERMANOVA on Bray-Curtis dissimilarity metrics), in contrast to the *H. polygyrus* experiments, which may relate to the differences in samples analyzed (cecum vs. feces) or the length of study (28 vs 49 days). Despite this, we once more noted a non-significant trend for a relative enrichment of *T. sanguinis* in uninfected, PAC-dosed mice (Figure 6c) despite a significant reduction in PAC-dosed mice during *T. muris* infection, again suggesting that infection abrogated the effects of PAC as was observed also for *H. polygyrus* infection ($p = 0.05$ for interaction between diet and infection by two-way ANOVA; Figure 6c). Interestingly, we also found that the combination of PAC and *T. muris* infection led to the expansion of zOTUs corresponding to the *Escherichia fergusonii* which was absent in all other treatment groups ($p < 0.01$ for interaction between diet and infection by two-way ANOVA; Figure 6c). Given that the expansion of the *Escherichia* genus in the mouse GM is often indicative of a dysbiotic GM,[44] our data suggest that the intake of PAC together with SSD may be a risk factor for *T. muris*–induced dysbiosis compared to SSD consumption alone. Of note, this is consistent with some of our immunological data (e.g. IL-6 production), suggesting that the administration of PAC to SSD-fed, *T. muris*-infected mice may increase parameters associated with inflammation. Collectively, these data indicate that significant interactions exist between gut parasites and dietary PAC on GM composition.

Trichuris muris infection changes the profile of microbial metabolites derived from proanthocyanidins

Given that helminth infection appeared to influence how the GM responded to PAC supplementation, we next assessed how *T. muris* and PAC may interact to influence the production of GM-derived metabolites. To this end, fecal samples of uninfected and *T. muris*-infected mice administered PAC were analyzed for short chain fatty acid (SCFA) concentrations. We observed significant interactions ($p < 0.05$) between PAC intake and infection for acetic acid, propionic acid, and total SCFA. These interactions reflected a generally higher level of SCFA in either uninfected PAC-dosed mice or *T. muris*-infected control mice, but a lower level in the combinatorial group of PAC-dosed *T. muris*-infected mice (Figure 7a). Thus, whilst both treatments in isolation promoted SCFA production, instead of an additive effect we detected an antagonistic trend. Butyric acid followed the same trend but was not significant (Figure 7a).

Several studies have shown that absorption of PAC in the small intestinal is minimal, while they are readily metabolized by the residing GM in the

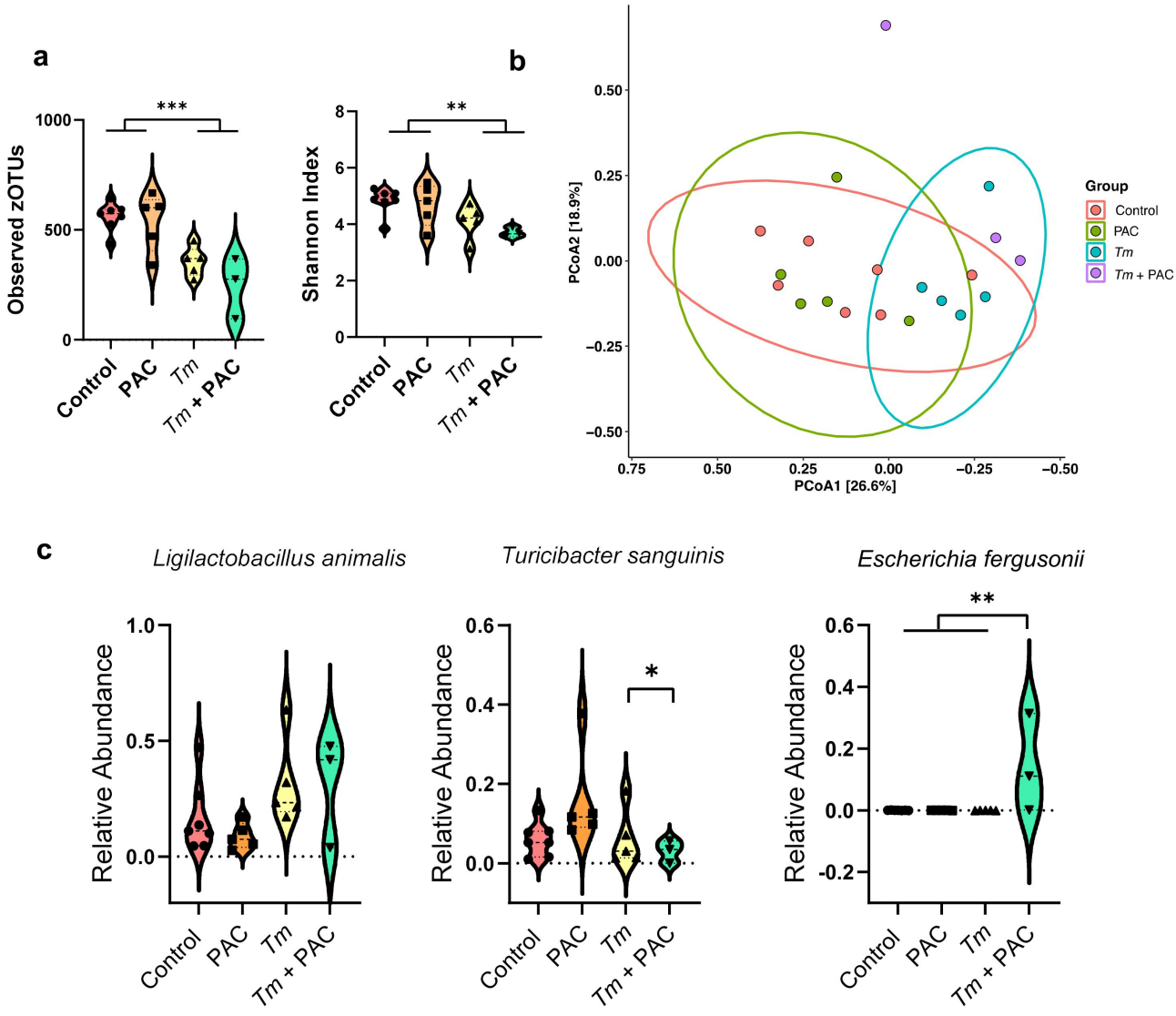

Figure 6. Impact of Trichuris muris (Tm) infection and proanthocyanidins (PAC) on the host fecal microbiota. a) Violin plots illustrating the number of observed zOTUs and Shannon Diversity Index for each treatment group. *** $p < 0.001$, ** $p < 0.01$ by two-way ANOVA followed by Tukey post-hoc testing. Shown is median and interquartile range. b) Principal coordinates analysis based on Bray-Curtis dissimilarity metrics for control and *Tm*-infected mice fed with semi-synthetic diets and dosed with either PAC or water (control). Each data point on the PCoA plots indicate a sample, with ellipses showing 95% confidence interval. The percentage in brackets is the percentage of variation explained by each PCoA axis. No ellipse was drawn for the *Tm*-infected mice dosed with PAC group as $n = 3$. Pairwise comparisons between treatment groups were performed using permutation MANOVAs on a distance matrix with p-value correction using the Holm method. $p<0.05$ was considered as significant. c) Relative abundance violin plots for zOTUs corresponding to *Ligilactobacillus animalis, Turicibacter sanguinis*, and *Escherichia fergusonii* in uninfected and *T. muris*-infected mice dosed with either PAC or water (control) ($n = 3$-7 per treatment group). **$p < 0.01$, *$p < 0.05$ by Tukey post-hoc testing following two-way ANOVA. Shown is median and interquartile range.

large intestine. Accordingly, PAC-derived phenolic metabolites such as phenyl-γ-valerolactones have been proposed to play a role in their putative health benefits, such as improved vascular function.[45,46] Therefore, we used targeted metabolomics to examine whether phenolic metabolites produced from the breakdown of PAC were altered during *T. muris* infection, by quantifying the abundance of a panel of PAC-derived metabolites in the cecum of uninfected and *T. muris*-infected mice dosed with PAC. As expected, PAC supplementation resulted in substantial increases of these metabolites in the cecum, compared to control-fed mice. Most of the metabolites were similar in both groups of mice that received PAC supplementation, regardless of infection (Figure 7b). However, we identified

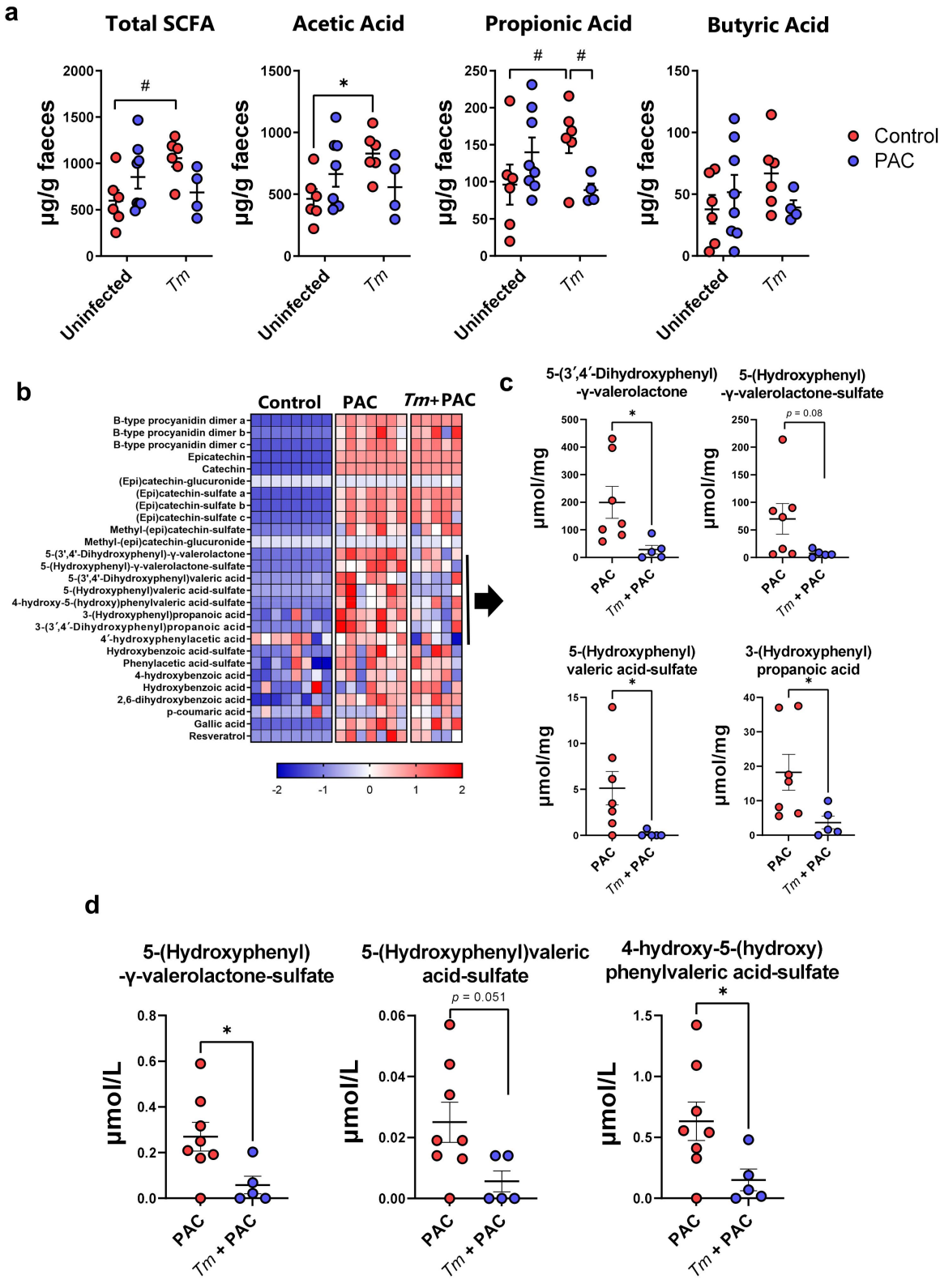

Figure 7. Short chain fatty acids and identification of proanthocyanidin metabolites in Trichuris muris infected mice. a) Effect of proanthocyanidins (PAC) and *Trichuris muris* (Tm) infection on the concentrations of total short chain fatty acids (SCFA), acetic acid, propionic acid, and butyric acid in fecal samples. A significant ($p < 0.05$) interaction between diet and infection was noted for acetic acid, propionic acid and total SCFA by two-way ANOVA. *$p < 0.05$, # $p = 0.06$ by Tukey's post-hoc test. b) Identification of PAC metabolites in the cecum of PAC-dosed uninfected and *T. muris*-infected mice relative to uninfected mice dosed with water. c) Caecal and d) serum concentrations of PAC-derived metabolites in PAC-dosed uninfected and *T. muris* infected mice. *$p < 0.05$ by unpaired t-test. $n = 5$-8 per group, pooled from two independent experiments. Shown are means ± S.E.M.

a cluster of related metabolites where abundance was reduced in infected mice. These were mostly phenyl-γ-valerolactones and phenylvaleric acid derivatives including 5-(3′,4′-dihydroxyphenyl)-γ-valerolactone, 5-(hydroxyphenyl)-γ-valerolactone-sulfate, 5-(hydroxyphenyl)valeric acid-sulfate, and 3-(hydroxyphenyl)propionic acid (Figure 7c). Moreover, the serum concentration of 5-(hydroxyphenyl)-γ-valerolactone-sulfate and 4-hydroxy-5-(hydroxyphenyl)valeric acid-sulfate were also significantly reduced in infected mice dosed with PAC (Figure 7d). 3-(Hydroxyphenyl)propionic acid and 5-(3′,4′-dihydroxyphenyl)-γ-valerolactone were not detected in the serum in any of the treatment groups (data not shown). Thus, both *T. muris* and PAC supplementation in isolation appeared to have positive effects on the production of microbial-derived metabolites in the gut, but concurrent infection and PAC intake attenuated both SCFA levels and the production and absorption of phenyl-γ-valerolactones, suggestive of an antagonistic interaction that may have a negative effect on tissue homeostasis and intestinal health.

Discussion

Whilst the immunomodulatory effects of parasites have been extensively demonstrated in previous studies, our understanding of the interactions between infection and bioactive dietary components remains limited.[47,48] Similarly, despite numerous investigations into the impact of helminth infection on the GM, diet-parasite interactions and their effects on gut health are largely unexplored.[39,49,50] Several studies have demonstrated strong anti-inflammatory properties of PAC, which have also been shown to be advantageous for gut health by supporting mucosal barrier function.[6,51] Moreover, PAC may alter the bacterial flora of the intestinal tract and thereby indirectly stimulate gut-associated lymphoid tissues, thus modulating *T*- or B-cell mediated immune responses.[52–56]

Based on these known anti-inflammatory and immunomodulatory properties, we hypothesized that PAC may reduce helminth-induced inflammation by either enhancing the diversity and composition of the GM, or by directly stimulating mucosal immune cells. Both infection models clearly showed a higher number of MLN cells in infected mice dosed with PAC, which suggests a strong effect of PAC on immune reactivity and lymphocyte proliferation. However, we found inconsistent effects of PAC on the immune polarization during *H. polygyrus* infection, but a clear trend for increased production of pro-inflammatory components, such as IL-6 and genes downstream of interferon signaling, in the immune response of PAC-treated mice during *T. muris* infection. The differences between the models may relate to the duration of the experiments, the different tissue location of the two parasites, or perhaps intrinsic differences in the host-parasite relationships. However, it was notable that, in the absence of infection, PAC had a much stronger effect on the cecal transcriptional response than the small intestinal response, which may suggest that the large intestine is more responsive to plant-derived phytochemicals such as polyphenols.

As PAC are known to be metabolized in the large intestines, we sought to identify which PAC metabolites were present in the cecum. As expected, several PAC metabolites were identified in PAC-treated mice. However, significantly fewer metabolites were found in *T. muris* infected mice dosed with PAC, including valerolactones. This may be closely related to the changes in the GM composition induced by helminth infection, which may alter PAC metabolism efficiency. Another suggestion could be that PAC metabolites are more easily absorbed in the gut, due to the increased permeability and disruption of the gut mucosal barrier caused by the helminth infections. However, the serum concentration of valerolactones was also significantly lower in infected mice, suggesting that impaired production of these metabolites by the GM seems most plausible.

We found that PAC had subtle changes on the mouse GM, with a consistent feature the enrichment of the *Turicibacter* genus, of which *T. sanguinis* is the most well-characterized species. *T. sanguinis* is a strictly anaerobic bacterium that may play a role in modulating host lipid metabolism and host body weight.[57] However, concurrent infection with either *H. polygyrus* or *T. muris* substantially suppressed *T. sanguinis* abundance,

suggesting a strong modifying effect of infection on PAC-induced changes in the GM composition and function, consistent with the suppressive effect of *T. muris* on PAC-derived metabolites. Interestingly, we also found the expansion of bacteria form the *Escherichia* genus in PAC-dosed mice infected with *T. muris*, but not *T. muris* fed SSD alone. This agrees with our recent data showing that fortification of SSD with inulin (a prebiotic oligosaccharide) also enables a pronounced dysbiosis in *T. muris*-infected mice (characterized by high *Escherichia* spp. abundance), whereas infected mice fed SSD alone had only minor GM changes and no *Escherichia* spp. expansion.[31] Overall, our results suggest an inter-relationship whereby helminth infection may abrogate PAC-induced changes in the GM, and PAC intake may enable some aspects of helminth-induced dysbiosis. This interaction between gut parasites and phytonutrient intake may have important implications for the assessment of the health-promoting effects of dietary additives where enteric infections may be present.

Semi-synthetic diets resemble Western-style diets that lack crude fibrous plant components such as pectin, lignin, and (poly)phenols. The consumption of such diets also often contains elevated levels of fat and simple sugars and is associated with the development of diseases such as obesity and colitis. It has been shown that incorporation of plant-derived fibers or phytochemicals such as PAC into refined, high fat diets can be protective against disease in mice.[34,58] However, the inclusion of high levels of fermentable fibers in refined diets has been shown to also have some detrimental effects, such as worsening of acute inflammation deriving from colitis induced by chemicals (DSS)[38] or infectious agents (*C. rodentium*).[59] Notably, we have recently shown that high levels of dietary inulin also impaired immunity to *T. muris*, with higher worm burdens and a Th1 driven immune response, indicating an important context-dependent immunological effect of fermentable fiber.[60] Together with our current results, this suggests that caution must be exercised when fortifying refined diets with high levels of phytochemicals during active enteric inflammation or infection. Indeed, mouse chow, which contains a high level of crude, unrefined plant fiber, also substantially increased *T. muris* burdens relative to purified diets, suggesting a continuum whereby increasing the concentration of prebiotic substrates progressively increases susceptibility to parasites. Thus, whilst the well-known health benefits of PAC or other plant fibers are clear, their immunomodulatory effects may differ according to context.

Overall, it can be speculated that diets containing little plant material or fermentable fibers seem to promote resistance to parasite infection in mice, whilst feeding unrefined chow or the addition of purified fibers such as inulin or pectin to SSD progressively down-regulates type-2 immunity to *T. muris* infection and instead promotes more of a type-1 immune response characterized by interferon production.[31,61] Thus, the production of hitherto undefined GM-derived metabolites likely shapes the propensity of immune cells to diverge away from type-2 functionality to either type-1 or T-regulatory responses, which may, in some cases, predispose to enteric infections and dysbiosis. In this current work, we have additionally demonstrated that the addition of the phytochemical PAC to SSD-based diets also tends to increase gene pathways related to interferon production in cecal tissue, and cause the expansion of pathobionts in the GM during *T. muris* infection. Thus, while our results and others clearly indicate that even if PAC and other phytonutrients have demonstrated beneficial health effects in the absence of gut pathogens, further studies should aim at unraveling the immunological mechanisms underlying this complex relationship between diet and immune function during infection with gastrointestinal parasites.

Material and methods

Proanthocyanidins

PAC derived from grape (*Vitus vinifera)* consisting of a mixture of oligomers and polymers were used for all experiments. For *H. polygyrus* experiments, PAC were derived from grape pomace and obtained by series of extraction and sephadex separation LH-20 gel chromatography as described previously.[62] The PAC had a mean degree of polymerization of 7.5. PAC used for the *T. muris* study were a commercial preparation derived from grape seed (Bulk Powders, Denmark), with a mean degree of polymerization of 4.2. Purity of both preparations was > 95% as determined by LC-DAD-MS and LC-DAD-MS/MS analyses.[63]

Parasites

H. polygyrus and *T. muris* were propagated, and excretory/secretory (E/S) antigens produced, as described previously.[60,64]

Mouse experiments

6-week-old C57/BL6 female mice were used in all experiments. Mice were fed a purified, semi-synthetic control diet (E15051–04, Ssniff, Germany, composition in Supplementary Table S1) throughout the entire study period, or, where indicated, standard rodent chow (D30, SAFE, France). All mice were given 1 week acclimatization, were monitored daily and weighed once a week. The mice were subjected to a 12 h light/dark cycle (6:00 a.m. to 6:00 p.m.) with *ad libitum* access to water and food, and randomly assigned to treatment groups. For *H. polygyrus* experiments, mice were orally gavaged on alternate days for 4 weeks with either PAC dissolved in sterile water (200 mg/kg BW, PAC, or *H. polygyrus* + PAC groups) or water (control and *H. polygyrus* groups). Mice were infected with *H. polygyrus* (200 third-stage larvae/mouse in 200 µl water) on day 14 and were humanely euthanized on day 28 (i.e., 14 days p.i.). For *T. muris* experiments, all mice were orally gavaged on alternate days for 7 weeks with either PAC (300 mg/kg body weight, PAC and *T. muris* + PAC groups) or water only (control and *T. muris* groups). After 2 weeks of PAC treatment, the appropriate treatment groups were infected with 20 eggs of *T. muris* on day 0, 14 and 28 to establish naturally occurring chronic infection,[65] before termination at day 35 post-first infection. Alternatively, mice were given a single dose of 300 *T. muris* eggs and killed at day 21 post-infection. All mice were humanely euthanized by cervical dislocation.

Sample collection

Fecal samples and blood were collected at necropsy. Separated serum was stored at −20°C until use. After sacrifice, the MLN were dissected and stored on ice in 10% fetal calf serum (FCS)-supplemented RPMI 1640 media (complete media) until further processing for flow cytometry. Cecal contents were harvested and cooled immediately on ice and stored at − 80°C until used for extraction. Tissue samples from the duodenum of *H. polygyrus* infected mice, and the cecal tip of *T. muris* infected mice, were collected and stored in RNA later. Full-thickness duodenum samples were collected from *H. polygyrus*-infected mice for histology. Histology samples were longitudinally opened, gently rinsed with PBS, and stored in 4% paraformaldehyde until further processing. Worm burdens were assessed by manual enumeration under a stereomicroscope.

Immunohistochemistry

Samples stored in 4% paraformaldehyde were embedded in paraffin blocks, sectioned, and mounted on glass slides. Mcpt1-positive mast cells were stained in paraffin-embedded sections, which were de-waxed, and antigen retrieval was performed with citrate buffer. Tissue sections were incubated with rat anti-mouse primary monoclonal mast cell protease-1 (MCPT-1) Ab (1:100, clone RF6.1; Thermo Fisher Scientific), followed by secondary staining with biotinylated rabbit anti-rat IgG (Abcam). Mcpt1$^+$ cells were manually enumerated by a microscopist blinded to the treatment groups.

Isolation of mesenteric lymph node cells

MLN were carefully dissected and trimmed of fat. Single cell suspensions were prepared by passing through a 70 µM cell strainer. Afterwards, the cell suspension was centrifuged at 450**g** for 5 min at room temperature. Cell counts and viability were assessed manually using a haematocytometer and trypan blue staining.

Flow cytometry, ex vivo cell stimulation and cytokine analysis

MLN cell suspensions were incubated with Fc-block (anti-CD16/CD32, BD Biosciences, cat no. 553142) followed by staining with antibodies against surface and intranuclear markers. Cells were kept at 4°C throughout the staining procedure. Cell surface markers were stained for 20 min using an antibody cocktail containing; FITC-conjugated hamster anti-mouse TCRβ

(clone H57–597; BD Biosciences, cat no. 553171), and PerCP-Cy5.5-conjugated rat anti-CD4 (RM4–5; BD Biosciences cat no.550954). For intranuclear (GATA-3 and T-bet) staining, FoxP3/Transcription Factor staining buffer (eBiosciences, 00-5523-00) was used according to manufacturer's instructions. Fixed/permeabilized cells were incubated for 30 min on ice with: Alexa Fluor® 647-conjugated mouse anti-mouse T-bet (4B10; BD Biosciences cat no. 561264), PE-conjugated rat anti-mouse GATA3 (TWAJ; Thermo Fisher Scientific cat no. 12-9966-42), FITC-conjugated rat anti-mouse FoxP3 (FJK-16s; Thermo Fisher Scientific cat no. 11-5773-82). Cells were analyzed on an BD Accuri C6 flow cytometer (BD Biosciences). All data were acquired and analyzed using Accuri CFlow Plus software (Accuri® Cytometers Inc.). Gating strategy is shown in Supplementary Figure 8.

For cytokine analysis, MLN cells were plated in triplicate into 96-well cell culture plates at the density of 5.0×10^6 cells/mL in complete media and stimulated with *T. muris* E/S antigens (50 µg/mL) or PBS. Cells were incubated at 37°C/5% CO_2 and cell-free supernatants were harvested after 24 h and stored at −20°C for subsequent analyses. Secreted cytokines were measured using a BD Th1/Th2/Th17 cytometric bead array (CBA) kit (BD Biosciences cat no. 560485) according to manufacturer's instructions. Samples were processed on a BD Accuri C6 flow cytometer (BD Biosciences), with data acquired using Accuri CFlow Plus software (Accuri® Cytometers Inc., MI, USA). In addition, IL-6 production decipted in Figure 4 was assessed by ELISA (Mouse IL-6 DuoSet, R and D Systems, UK).

Enzyme-linked immunosorbent assay

T. muris E/S-specific antibodies were measured from diluted (1:50) serum using a previously described ELISA protocol.[60] The antibodies employed for ELISA were biotin-conjugated rat anti-mouse IgG2a (clone R19-5, BD Biosciences, Denmark cat no. 550332) and anti-mouse IgG conjugated to horseradish peroxidase (HRP; Bio-Rad, Germany cat no. 1706516). Absorbance was measured at an optical density of 450 nm with a Multiskan FC plate reader (Waltham, MA, USA). *H. polygyrus* E/S-specific IgG1 was detected using goat anti-mouse IgG1-HRP conjugate (Invitrogen, cat no. A10551).

RNA extraction, RNA-sequencing, and qPCR

Tissue was mechanically homogenized in QIAzol lysis buffer using a gentleMACS™ dissociator (Miltenyi Biotec, Germany) and total RNA was isolated using miRNeasy Mini Kits (Qiagen, CA, USA) as per manufacturer's instructions. Total RNA concentrations were determined using a NanoDrop ND-1000 spectrophotometer (NanoDrop Technologies, DE, USA). Paired-end (100 bp) RNA-sequencing was carried out using the DNBSEQ sequencing platform (BGI, Copenhagen, Denmark). Clean reads were mapped to the mouse genome (mm10) using Bowtie2 (v2.2.5). Differentially expressed genes were detected using DEseq2.[66] cDNA was synthesized from 500 ng of RNA using Quantitect Reverse Transcriptase kits (Qiagen), and qPCR was performed using perfeCTa SYBR green fastmix (Quanta Bioscience) using the following program: 95°C for 2 min followed by 40 cycles of 15 s at 95°C and 20 s at 60°C. Primer sequences are listed in Supplementary Table S2.

Short chain fatty acids and proanthocyanidin metabolites analysis

SCFA were measured by GC-FID using the same methodology as described by Choi et al.,[67] whilst PAC metabolites were analyzed using UHPLC-QToF using previous described methods. For PAC metabolites analysis, sample preparation of plasma was done according to the protocol of Dudonné et al.[68] For the cecum, samples were freeze-dried before being extracted with 25 µL per mg of dry matter of methanol:water (50:50 v/v) spiked with 0.5 ppm of 4-hydroxybenzoic acid-d_4. Samples were homogenenized for 2 min with a Bead Rupter12 (Omni International, Kennesaw, GA, USA), vortexed during 5 min, sonicated for 30 min at room temperature and re-vortexed during 5 min. Before injection, samples were centrifuged at 18 000 g during 30 min at 4°C before being filtered through

a 0.22 µm Nylon filter. PAC metabolites analysis was carried out with an Acquity I-Class UHPLC coupled with a Synapt G2-Si (Waters, Milford, MA) using the UHPLC-QToF method from Lessard-Lord et al.[69] PAC and (epi)catechin derivatives were quantified as epicatechin equivalent and PAC metabolites as 5-(3′,4′-dihydroxyphenyl)-γ-valerolactone equivalent, while gallic acid was quantified with its own standard.

Microbiota analysis

DNA extraction and amplification of the 16S rRNA gene V3 region

DNA was extracted from 100 mg cecal content (*H. polygyrus* study) and fecal samples (*T. muris* study) using the Bead-Beat Micro AX Gravity kit (A&A Biotechnology, Poland) as per manufacturer's instructions with the addition of mutanolysin and lysozyme to enhance the bacteria lysis yield. The concentration of DNA was assessed utilizing the Qubit® dsDNA HS Assay Kit (Life Technologies, CA, USA) and measurement was taken using the Varioskan Flash Multimode Reader (Thermo Fisher Scientific, MA, USA). Library was prepared through a two-step PCR process. In the initial PCR step, the 16S rRNA gene V3 region was amplified using the Nextera Index Kit (Illumina, CA, USA) compatible forward primer nxt388_F:(5'-TCGTCGGCAG CGTCAGATGT GTATAAGAGA CAGACWCCTA CGGGWGG CAGCAG-3') and reverse primer nxt518_R:(5'-GTCTCGTGGG CTCGGAGATG TGTATAA GAG ACAGATTACC GCGGCTGCTGG-3'). This step utilized a final reaction volume of 25 µl/sample, incorporating 5 µl of 5 × PCRBIO HiFi buffer (PCR Biosystems©, UK), 0.25 µl of PCRBIO HiFi Polymerase (PCR Biosystems©, UK), 0.5 µl of primer mix (10 µM, nxt_388_F and nxt_518_R), 5 µl of genomic DNA (5ng/µl), and was adjusted to 25 µl with nuclease-free water. Reaction conditions included an initial denaturation at 95°C for 2 min, followed by 33 cycles of: 95°C for 15 seconds, 55°C for 15 seconds and 72°C for 20 seconds, and a final extension step at 72°C for 4 min. A second PCR step was conducted, involving 5 µl of 5 × PCRBIO HiFi buffer (PCR Biosystems©, UK), 0.25 µl of PCRBIO HiFi Polymerase (PCR Biosystems©, UK), 2 µl of each P5 and P7 primer (Nextera Index Kit, Illumina, CA, USA), 2 µl of initial PCR product, and additional nuclease-free water to make up a total volume of 25 µl. Reaction parameters of PCR2 consisted of an initial denaturation at 95°C for 1 min, followed by 13 cycles of: 95°C for 15 s, 55°C for 15 s and 72°C for 15 s, and a final extension step at 72°C for 5 min. The second PCR products were cleaned up using SpeedBeads™ magnetic carboxylate (obtained from Sigma Aldrich). Cleaned PCR2 products were quantified using Qubit® dsDNA HS Assay Kit (Life Technologies, CA, USA) and then mixed equimolarly. High-throughput sequencing of 16S rRNA gene amplicon (V3 region) was done, using a NextSeq550 platform (Illumina, San Diego, CA, USA) with the Mid Output Kit v2 (300 cycles), to determine the bacterial composition of cecal and fecal contents.

Data processing and analysis

The merging and trimming of raw dataset containing pair-ended reads with corresponding quality scores were carried out using *fastq_mergepairs* and *fastq_filter* scripts implemented in the VSEARCH pipeline[70] utilizing the specified settings: -fastq_minovlen 100, -fastq_maxee 2.0 -fastq_truncqual 4 -fastq_minlen 150. Removal of chimeric reads from dataset and constructing zero-radius operational taxonomical units (zOTUs) were performed by using UNOISE3 in VSEARCH pipeline. The Greengenes (13.8)[71] 16S rRNA gene collection was used as a reference database and taxonomical assignments were obtained by using SINTAX[72] for the 16S rRNA gene database.

zOTUs belonging to bacteria assigned at phylum level was included in analysis. Unassigned taxonomy names at any levels lower than phylum were adjusted to be termed as "Unclassified *lowest taxonomy name*". zOTUs mapped to *Cyanobacteria*/Chloroplast were excluded prior to the analysis. The taxonomy names of zOTUs previously belonging to the genus *Lactobacillus* were updated manually following the announcement of Zheng et al.[73]

The analysis and visualization of data from the two studies conducted for each infection model were performed independently in RStudio using R version 4.2.1 and R packages phyloseq,[74] DESeq2,[66] tidyverse,[75] reshape2,[76] pheatmap,[77] and RColorbrewer.[78] Alpha and beta diversity

analyses were performed on rarefied data (7000 reads/sample). Alpha diversity was assessed by observed zOTUs and Shannon Index metrics, while beta diversity was evaluated through principal coordinates analysis (PCoA) with Bray – Curtis dissimilarity metrics. A DESeq2 analysis was conducted to determine species level differentially abundant bacteria between treatments and DESeq2-based heatmap was plotted to show significantly differentially abundant bacteria with an adjusted *p* value below a threshold of 0.05. In addition, within each study, bar plots were drawn to show how the relative abundance of selected bacteria identified by DESeq2 changed among some of the treatment groups.

For beta diversity, pairwise comparisons between treatment groups within each study were conducted by using permutation MANOVAs on a distance matrix with Holm *p* value adjustment method using the *pairwise.perm.manova* function available in R RVAideMemoire package.[79] In DESeq2 analysis, *p* values attained by the Wald test were corrected by using the Benjamini and Hochberg method by default, and adjusted *p* value threshold of below 0.05 was considered as significant.

Statistical analysis

Statistical analyses were performed in Prism 8.0.2 (GraphPad Software). Assumptions of normality were checked through Shapiro-Wilk tests, or inspection of histogram plots and Kolmogorov-Smirnov tests of ANOVA residuals. Parametric data were analyzed using unpaired t-tests, or ANOVA followed by Tukey post-hoc testing, and presented as means ± S.E.M. Non-parametric data were analyzed using Mann-Whitney tests or Kruskal-Wallis and Dunn's post hoc tests, and results presented as median values. Details of each experiment are given in the appropriate figure legends.

Acknowledgments

The authors would like to thank Mette Marie Arnt Schjelde and Penille Jensen for excellent laboratory assistance and support for the conduction of animal studies. We are grateful to Rick Maizels (University of Glasgow) and Sebastian Rausch (Freie University, Berlin), for provision and advice on *H. polygyrus* infections. This work was funded by Independent Research Fund Denmark (Grant # 702649B).

Disclosure statement

No potential conflict of interest was reported by the author(s).

Funding

The work was supported by the Independent Research Fund Denmark [702649B].

ORCID

Dennis Sandris Nielsen http://orcid.org/0000-0001-8121-1114
Andrew R. Williams http://orcid.org/0000-0002-8231-282X

Data availability statement

RNA sequence data from cecum and duodenum are deposited at the NCBI Gene Expression Omnibus (GEO: Accession numbers GSE174756 and GSE176182). The raw 16S rRNA sequencing data can be accessed at Sequence Read Archive (https://www.ncbi.nlm.nih.gov/sra) using the accession number PRJNA1044063.

Ethical statement

Mice experiments were approved by the Danish Animal Experiment Inspectorate (Ref. No. 2015-15-0201–00760) and performed in accordance with EU Directive 2010/63/EU for animal experiments.

References

1. Tao W, Zhang Y, Shen X, Cao Y, Shi J, Ye X, Chen S. Rethinking the Mechanism of the Health Benefits of Proanthocyanidins: Absorption, Metabolism, and Interaction with Gut Microbiota. Compr Rev Food Sci Food Saf. 2019;18(4):971–985. doi:10.1111/1541-4337.12444 .
2. Akaberi M, Hosseinzadeh H. Grapes (Vitis vinifera) as a Potential Candidate for the Therapy of the Metabolic Syndrome. Phytother Res. 2016;30(4):540–556. doi:10.1002/ptr.5570.
3. Williams AR, Klaver EJ, Laan LC, Ramsay A, Fryganas C, Difborg R, Kringel H, Reed JD, Mueller-Harvey I, Skov S, et al. Co-operative suppression of inflammatory responses in human dendritic cells by

plant proanthocyanidins and products from the parasitic nematode Trichuris suis. Immunology. 2017;150 (3):312–328. doi:10.1111/imm.12687.
4. Ahmad SF, Zoheir KM, Abdel-Hamied HE, Ashour AE, Bakheet SA, Attia SM, Abd-Allah ARA. Grape seed proanthocyanidin extract has potent anti-arthritic effects on collagen-induced arthritis by modifying the T cell balance. Int Immunopharmacol. 2013;17 (1):79–87. doi:10.1016/j.intimp.2013.05.026.
5. Miyake M, Sasaki K, Ide K, Matsukura Y, Shijima K, Fujiwara D. Highly oligomeric procyanidins ameliorate experimental autoimmune encephalomyelitis via suppression of Th1 immunity. J Immunol (Baltimore, Md: 1950) 2006;176(10):5797–5804. doi:10.4049/jimmunol.176.10.5797.
6. Gil-Cardoso K, Comitato R, Ginés I, Ardévol A, Pinent M, Virgili F, Terra X, Blay M. Protective effect of proanthocyanidins in a rat model of mild intestinal inflammation and impaired intestinal permeability induced by LPS. Mol Nutr Food Res. 2019;63(8): e1800720. doi:10.1002/mnfr.201800720.
7. Anhê FF, Roy D, Pilon G, Dudonné S, Matamoros S, Varin TV, Garofalo C, Moine Q, Desjardins Y, Levy E, et al. A polyphenol-rich cranberry extract protects from diet-induced obesity, insulin resistance and intestinal inflammation in association with increased Akkermansia spp. population in the gut microbiota of mice. Gut. 2015;64(6):872–883. doi:10.1136/gutjnl-2014-307142.
8. Han M, Song P, Huang C, Rezaei A, Farrar S, Brown MA, Ma X. Dietary grape seed proanthocyanidins (GSPs) improve weaned intestinal microbiota and mucosal barrier using a piglet model. Oncotarget. 2016;7(49):80313–80326. doi:10.18632/oncotarget.13450.
9. Lee JY, Wasinger VC, Yau YY, Chuang E, Yajnik V, Leong RW. Molecular pathophysiology of epithelial barrier dysfunction in inflammatory bowel diseases. Proteomes. 2018;6(2):6. doi:10.3390/proteomes6020017.
10. Nallathambi R, Poulev A, Zuk JB, Raskin I. Proanthocyanidin-rich grape seed extract reduces inflammation and oxidative stress and restores tight junction barrier function in Caco-2 colon cells. Nutrients. 2020;12(6):12. doi:10.3390/nu12061623.
11. Denis MC, Desjardins Y, Furtos A, Marcil V, Dudonné S, Montoudis A, Garofalo C, Delvin E, Marette, A, Levy E. Prevention of oxidative stress, inflammation and mitochondrial dysfunction in the intestine by different cranberry phenolic fractions. Clin Sci. 2015;128(3):197–212.
12. Liu W, Zhao S, Wang J, Shi J, Sun Y, Wang W, Ning G, Hong J, Liu R. Grape seed proanthocyanidin extract ameliorates inflammation and adiposity by modulating gut microbiota in high-fat diet mice. Mol Nutr Food Res. 2017;61(9):61. doi:10.1002/mnfr.201601082.
13. Tzounis X, Rodriguez-Mateos A, Vulevic J, Gibson GR, Kwik-Uribe C, Spencer JP. Prebiotic evaluation of cocoa-derived flavanols in healthy humans by using a randomized, controlled, double-blind, crossover intervention study. Am J Clin Nutr. 2011;93(1):62–72. doi:10.3945/ajcn.110.000075.
14. Gil-Cardoso K, Ginés I, Pinent M, Ardévol A, Blay M, Terra X. Effects of flavonoids on intestinal inflammation, barrier integrity and changes in gut microbiota during diet-induced obesity. Nutr Res Rev. 2016;29 (2):234–248. doi:10.1017/S0954422416000159.
15. Shi N, Li N, Duan X, Niu H. Interaction between the gut microbiome and mucosal immune system. Mil Med Res. 2017;4(1):14. doi:10.1186/s40779-017-0122-9.
16. Mowat AM. Anatomical basis of tolerance and immunity to intestinal antigens. Nat Rev Immunol. 2003;3 (4):331–341. doi:10.1038/nri1057.
17. Blander JM, Longman RS, Iliev ID, Sonnenberg GF, Artis D. Regulation of inflammation by microbiota interactions with the host. Nat Immunol. 2017;18 (8):851–860. doi:10.1038/ni.3780.
18. Brestoff JR, Artis D. Immune regulation of metabolic homeostasis in health and disease. Cell. 2015;161 (1):146–160. doi:10.1016/j.cell.2015.02.022.
19. Loukas A, Maizels RM, Hotez PJ. The yin and yang of human soil-transmitted helminth infections. Int J Parasitol. 2021;51(13–14):1243–1253. doi:10.1016/j.ijpara.2021.11.001.
20. Charlier J, Thamsborg SM, Bartley DJ, Skuce PJ, Kenyon F, Geurden T, Hoste H, Williams AR, Sotiraki S, Höglund J, et al. Mind the gaps in research on the control of gastrointestinal nematodes of farmed ruminants and pigs. Transbound Emerg Dis. 2018;65:217–234. doi:10.1111/tbed.12707.
21. Cooper PJ. Mucosal immunology of geohelminth infections in humans. Mucosal Immunol. 2009;2 (4):288–299. doi:10.1038/mi.2009.14.
22. Maizels RM, Hewitson JP, Murray J, Harcus YM, Dayer B, Filbey KJ, Grainger JR, McSorley HJ, Reynolds LA, Smith KA, et al. Immune modulation and modulators in Heligmosomoides polygyrus infection. Exp Parasitol. 2012;132(1):76–89. doi:10.1016/j.exppara.2011.08.011.
23. Gerbe F, Sidot E, Smyth DJ, Ohmoto M, Matsumoto I, Dardalhon V, Cesses P, Garnier L, Pouzolles M, Brulin B, et al. Intestinal epithelial tuft cells initiate type 2 mucosal immunity to helminth parasites. Nature. 2016;529 (7585):226–230. doi:10.1038/nature16527.
24. Urban JF Jr., Katona IM, Paul WE, Finkelman FD. Interleukin 4 is important in protective immunity to a gastrointestinal nematode infection in mice. Proc Natl Acad Sci USA. 1991;88(13):5513–5517. doi:10.1073/pnas.88.13.5513.
25. Anthony RM, Rutitzky LI, Urban JF Jr., Stadecker MJ, Gause WC. Protective immune mechanisms in helminth infection. Nat Rev Immunol. 2007;7 (12):975–987. doi:10.1038/nri2199.
26. Williams AR, Krych L, Fauzan Ahmad H, Nejsum P, Skovgaard K, Nielsen DS, Thamsborg SM. A

polyphenol-enriched diet and Ascaris suum infection modulate mucosal immune responses and gut microbiota composition in pigs. PLOS ONE. 2017;12(10): e0186546. doi:10.1371/journal.pone.0186546.
27. Ramírez-Restrepo CA, Pernthaner A, Barry TN, López-Villalobos N, Shaw RJ, Pomroy WE, Hein WR. Characterization of immune responses against gastrointestinal nematodes in weaned lambs grazing willow fodder blocks. Anim Feed Sci Technol. 2010;155(2–4):99–110. doi:10.1016/j.anifeedsci.2009.10.006.
28. Forgie AJ, Gao Y, Ju T, Pepin DM, Yang K, Gänzle MG, Ozga JA, Chan CB, Willing BP. Pea polyphenolics and hydrolysis processing alter microbial community structure and early pathogen colonization in mice. J Nutr Biochem. 2019;67:101–110. doi:10.1016/j.jnutbio.2019.01.012.
29. Klementowicz JE, Travis MA, Grencis RK. Trichuris muris: a model of gastrointestinal parasite infection. Semin Immunopathol. 2012;34(6):815–828. doi:10.1007/s00281-012-0348-2.
30. Shea-Donohue T, Notari L, Stiltz J, Sun R, Madden KB, Urban JF Jr., Zhao A. Role of enteric nerves in immune-mediated changes in protease-activated receptor 2 effects on gut function. Neurogastroenterol Motil. 2010;22(10):1138–e291. doi:10.1111/j.1365-2982.2010.01557.x.
31. Israelson H, Vedsted-Jakobsen A, Zhu L, Gagnaire A, von Münchow A, Polakovicova N, Valente AH, Raza A, Andersen-Civil AIS, Olsen JE, et al. Diet composition drives tissue-specific intensity of murine enteric infections. mBio. 2024;0(2):e02603–23. doi:10.1128/mbio.02603-23.
32. Jang S, Sun J, Chen P, Lakshman S, Molokin A, Harnly JM, Vinyard BT, Urban JF, Davis CD, Solano-Aguilar G, et al. Flavanol-Enriched Cocoa Powder Alters the Intestinal Microbiota, Tissue and Fluid Metabolite Profiles, and Intestinal Gene Expression in Pigs. J Nutr. 2016;146(4):673–680. doi:10.3945/jn.115.222968.
33. Van Hul M, Geurts L, Plovier H, Druart C, Everard A, Ståhlman M, Rhimi M, Chira K, Teissedre P-L, Delzenne NM, et al. Reduced obesity, diabetes, and steatosis upon cinnamon and grape pomace are associated with changes in gut microbiota and markers of gut barrier. Am J Physiol Endocrinol Metab. 2018;314(4):E334–e52. doi:10.1152/ajpendo.00107.2017.
34. González-Quilen C, Rodríguez-Gallego E, Beltrán-Debón R, Pinent M, Ardévol A, Blay MT, Terra X. Health-Promoting Properties of Proanthocyanidins for Intestinal Dysfunction. Nutrients. 2020;12(1):130. doi:10.3390/nu12010130.
35. Xi R, Montague J, Lin X, Lu C, Lei W, Tanaka K, Zhang YV, Xu X, Zheng X, Zhou X, et al. Up-regulation of gasdermin C in mouse small intestine is associated with lytic cell death in enterocytes in worm-induced type 2 immunity. Proc Natl Acad Sci USA. 2021;118(30):118. doi:10.1073/pnas.2026307118.
36. Downing LE, Edgar D, Ellison PA, Ricketts ML. Mechanistic insight into nuclear receptor-mediated regulation of bile acid metabolism and lipid homeostasis by grape seed procyanidin extract (GSPE). Cell Biochem Funct. 2017;35(1):12–32. doi:10.1002/cbf.3247.
37. Sorobetea D, Svensson-Frej M, Grencis R. Immunity to gastrointestinal nematode infections. Mucosal Immunol. 2018;11(2):304–315. doi:10.1038/mi.2017.113.
38. Miles JP, Zou J, Kumar MV, Pellizzon M, Ulman E, Ricci M, Gewirtz AT, Chassaing B. Supplementation of low- and high-fat diets with fermentable fiber exacerbates severity of DSS-induced acute colitis. Inflamm Bowel Dis. 2017;23(7):1133–1143. doi:10.1097/MIB.0000000000001155.
39. Brosschot TP, Reynolds LA. The impact of a helminth-modified microbiome on host immunity. Mucosal Immunol. 2018;11(4):1039–1046. doi:10.1038/s41385-018-0008-5.
40. Reynolds LA, Smith KA, Filbey KJ, Harcus Y, Hewitson JP, Redpath SA, Valdez Y, Yebra MJ, Finlay BB, Maizels RM, et al. Commensal-pathogen interactions in the intestinal tract: lactobacilli promote infection with, and are promoted by, helminth parasites. Gut Microbes. 2014;5(4):522–532. doi:10.4161/gmic.32155.
41. Fung TC, Vuong HE, Luna CDG, Pronovost GN, Aleksandrova AA, Riley NG, Vavilina A, McGinn J, Rendon T, Forrest LR, et al. Intestinal serotonin and fluoxetine exposure modulate bacterial colonization in the gut. Nat Microbiol. 2019;4(12):2064–2073. doi:10.1038/s41564-019-0540-4.
42. Yokozawa T, Cho EJ, Park CH, Kim JH. Protective effect of proanthocyanidin against diabetic oxidative stress. Evidence-based complementary and alternative medicine: eCAM. Evidence-Based Complementary and Altern Med. 2012;2012:1–11. doi:10.1155/2012/623879.
43. Holm JB, Sorobetea D, Kiilerich P, Ramayo-Caldas Y, Estellé J, Ma T, Madsen L, Kristiansen K, Svensson-Frej M. Chronic Trichuris muris Infection Decreases Diversity of the Intestinal Microbiota and Concomitantly Increases the Abundance of Lactobacilli. PLOS ONE. 2015;10(5):e0125495. doi:10.1371/journal.pone.0125495.
44. Madjirebaye P, Peng F, Mueed A, Huang T, Mahamat B, Pahane MM, Xi Q, Chen X, Moussa K, Kadebe ZT, et al. Exploring Impact of Probiotic-Fermented Soymilk on Dextran-Sulfate-Sodium-Induced Ulcerative Colitis via Modulating Inflammation and Gut Microbiota Profile. Mol Nutr Food Res. 2024;68(5):e2300586. doi:10.1002/mnfr.202300586.
45. Rodriguez-Mateos A, Feliciano RP, Boeres A, Weber T, Dos Santos CN, Ventura MR, Heiss C. Cranberry (poly) phenol metabolites correlate with improvements in vascular function: A double-blind, randomized, controlled, dose-response, crossover study. Mol Nutr

Food Res. 2016;60(10):2130–2140. doi:10.1002/mnfr.201600250.
46. Montagnana M, Danese E, Angelino D, Mena P, Rosi A, Benati M, Gelati M, Salvagno GL, Favaloro EJ, Del Rio D, et al. Dark chocolate modulates platelet function with a mechanism mediated by flavan-3-ol metabolites. Medicine (Baltimore). 2018;97(49):e13432. doi:10.1097/MD.0000000000013432.
47. McSorley HJ, Maizels RM. Helminth infections and host immune regulation. Clin Microbiol Rev. 2012;25(4):585–608. doi:10.1128/CMR.05040-11.
48. Maizels RM, Yazdanbakhsh M. Immune regulation by helminth parasites: cellular and molecular mechanisms. Nat Rev Immunol. 2003;3(9):733–744. doi:10.1038/nri1183.
49. Houlden A, Hayes KS, Bancroft AJ, Worthington JJ, Wang P, Grencis RK, Roberts IS. Chronic Trichuris muris Infection in C57BL/6 Mice Causes Significant Changes in Host Microbiota and Metabolome: Effects Reversed by Pathogen Clearance. PLOS ONE. 2015;10(5):e0125945. doi:10.1371/journal.pone.0125945.
50. Su C, Su L, Li Y, Long SR, Chang J, Zhang W, Walker WA, Xavier RJ, Cherayil BJ, Shi HN, et al. Helminth-induced alterations of the gut microbiota exacerbate bacterial colitis. Mucosal Immunol. 2018;11(1):144–157. doi:10.1038/mi.2017.20.
51. Pierre JF, Heneghan AF, Feliciano RP, Shanmuganayagam D, Roenneburg DA, Krueger CG, Reed JD, Kudsk KA. Cranberry proanthocyanidins improve the gut mucous layer morphology and function in mice receiving elemental enteral nutrition. JPEN J Parenter Enteral Nutr. 2013;37(3):401–409. doi:10.1177/0148607112463076.
52. Smith AH, Mackie RI. Effect of condensed tannins on bacterial diversity and metabolic activity in the rat gastrointestinal tract. Appl Environ Microb. 2004;70(2):1104–1115. doi:10.1128/AEM.70.2.1104-1115.2004.
53. Casanova-Martí À, Serrano J, Portune KJ, Sanz Y, Blay MT, Terra X, Ardévol A, Pinent M. Grape seed proanthocyanidins influence gut microbiota and enteroendocrine secretions in female rats. Food Funct. 2018;9(3):1672–1682. doi:10.1039/C7FO02028G.
54. Zhou Y, Zhi F. Lower Level of Bacteroides in the Gut Microbiota is Associated with Inflammatory Bowel Disease: A Meta-Analysis. Biomed Res Int. 2016;2016:5828959. doi:10.1155/2016/5828959.
55. Provenza FD, Villalba JJ. The role of natural plant products in modulating the immune system: An adaptable approach for combating disease in grazing animals. Small Ruminant Res. 2010;89(2–3):131–139. doi:10.1016/j.smallrumres.2009.12.035.
56. Belkaid Y, Hand TW. Role of the microbiota in immunity and inflammation. Cell. 2014;157(1):121–141. doi:10.1016/j.cell.2014.03.011.
57. Lynch JB, Gonzalez EL, Choy K, Faull KF, Jewell T, Arellano A, Liang J, Yu KB, Paramo J, Hsiao EY, et al. Gut microbiota Turicibacter strains differentially modify bile acids and host lipids. Nat Commun. 2023;14(1):3669. doi:10.1038/s41467-023-39403-7.
58. Anhê FF, Pilon G, Roy D, Desjardins Y, Levy E, Marette A. Triggering Akkermansia with dietary polyphenols: A new weapon to combat the metabolic syndrome? Gut Microbes. 2016;7(2):146–153. doi:10.1080/19490976.2016.1142036.
59. An J, Zhao X, Wang Y, Noriega J, Gewirtz AT, Zou J, Baumler AJ. Western-style diet impedes colonization and clearance of Citrobacter rodentium. PLOS Pathog. 2021;17(4):e1009497. doi:10.1371/journal.ppat.1009497.
60. Myhill LJ, Stolzenbach S, Mejer H, Jakobsen SR, Hansen TVA, Andersen D, Brix S, Hansen LH, Krych L, Nielsen DS, et al. Fermentable dietary fiber promotes helminth infection and exacerbates host inflammatory responses. J Immunol. 2020;204(11):3042–3055. doi:10.4049/jimmunol.1901149.
61. Valente AH, Jensen KMR, Myhill LJ, Zhu L, Mentzel CMJ, Krych L, Simonsen HT, Castro-Mejía JL, Gobbi A, Bach Knudsen KE, et al. Dietary non-starch polysaccharides impair immunity to enteric nematode infection. BMC Biol. 2023;21(1):138. doi:10.1186/s12915-023-01640-z.
62. Andersen-Civil AIS, Leppä MM, Thamsborg SM, Salminen JP, Williams AR. Structure-function analysis of purified proanthocyanidins reveals a role for polymer size in suppressing inflammatory responses. Commun Biol. 2021;4(1):896. doi:10.1038/s42003-021-02408-3.
63. Andersen-Civil AIS, Myhill LJ, Büdeyri Gökgöz N, Engström MT, Mejer H, Zhu L, Zeller WE, Salminen J-P, Krych L, Lauridsen C, et al. Dietary proanthocyanidins promote localized antioxidant responses in porcine pulmonary and gastrointestinal tissues during Ascaris suum-induced type 2 inflammation. Faseb J. 2022;36(4):e22256. doi:10.1096/fj.202101603RR.
64. Valanparambil RM, Segura M, Tam M, Jardim A, Geary TG, Stevenson MM. Production and analysis of immunomodulatory excretory-secretory products from the mouse gastrointestinal nematode Heligmosomoides polygyrus bakeri. Nat Protoc. 2014;9(12):2740–2754. doi:10.1038/nprot.2014.184.
65. Glover M, Colombo SAP, Thornton DJ, Grencis RK, Gause WC. Trickle infection and immunity to Trichuris muris. PLOS Pathog. 2019;15(11):e1007926. doi:10.1371/journal.ppat.1007926.
66. Love MI, Huber W, Anders S. Moderated estimation of fold change and dispersion for RNA-seq data with DESeq2. Genome Biol. 2014;15(12):550. doi:10.1186/s13059-014-0550-8.
67. Choi BSY, Daniel N, Houde VP, Ouellette A, Marcotte B, Varin TV, Vors C, Feutry P, Ilkayeva O, Ståhlman M, et al. Feeding diversified protein sources exacerbates hepatic insulin resistance via increased gut microbial branched-chain fatty acids and mTORC1

signaling in obese mice. Nat Commun. 2021;12 (1):3377. doi:10.1038/s41467-021-23782-w.
68. Dudonné S, Dubé P, Pilon G, Marette A, Jacques H, Weisnagel J, Desjardins Y. Modulation of strawberry/cranberry phenolic compounds glucuronidation by co-supplementation with onion: Characterization of phenolic metabolites in rat plasma using an optimized μSPE–UHPLC-MS/MS method. J Agr Food Chem. 2014;62(14):3244–3256. doi:10.1021/jf404965z.
69. Lessard-Lord J, Plante P-L, Desjardins Y. Purified recombinant enzymes efficiently hydrolyze conjugated urinary (poly)phenol metabolites. Food Funct. 2022;13 (21):10895–10911. doi:10.1039/D2FO02229J.
70. Rognes T, Flouri T, Nichols B, Quince C, Mahé F. VSEARCH: a versatile open source tool for metagenomics. PeerJ. 2016;4:e2584. doi:10.7717/peerj.2584.
71. McDonald D, Price MN, Goodrich J, Nawrocki EP, DeSantis TZ, Probst A, Andersen GL, Knight R, Hugenholtz P. An improved Greengenes taxonomy with explicit ranks for ecological and evolutionary analyses of bacteria and archaea. ISME J. 2012;6 (3):610–618. doi:10.1038/ismej.2011.139.
72. Robert CE. SINTAX: a simple non-Bayesian taxonomy classifier for 16S and ITS sequences. bioRxiv 2016; 074161.
73. Zheng J, Wittouck S, Salvetti E, Franz C, Harris HMB, Mattarelli P, O'Toole PW, Pot B, Vandamme P, Walter J, et al. A taxonomic note on the genus Lactobacillus: Description of 23 novel genera, emended description of the genus Lactobacillus Beijerinck 1901, and union of Lactobacillaceae and Leuconostocaceae. Int J Syst Evol Microbiol. 2020;70(4):2782–2858. doi:10.1099/ijsem.0.004107.
74. McMurdie PJ, Holmes S, Watson M. phyloseq: an R package for reproducible interactive analysis and graphics of microbiome census data. PLOS ONE. 2013;8(4):e61217. doi:10.1371/journal.pone.0061217.
75. Wickham H, Averick M, Bryan J, Chang W, McGowan L, François R, Grolemund G, Hayes A, Henry L, Hester J. Welcome to the Tidyverse. J Open Source Softw. 2019;4(43):1686. doi:10.21105/joss.01686.
76. Wickham H. Reshaping Data with the reshape Package. J Stat Softw. 2007;21(12):1–20. doi:10.18637/jss.v021.i12.
77. Kolde R. Pretty heatmaps. 2019. https://cran.r-project.org/package=pheatmap.
78. Neuwirth E. ColorBrewer Palettes. 2014. https://cran.r-project.org/package=RColorBrewer.
79. Herve M. RVAideMemoire: Testing and Plotting Procedures for Biostatistics. 2021.